Summary of physicochemical properties of natural gas hydrate and associated gas-hydrate-bearing sediments, JAPEX/JNOC/GSC Mallik 2L-38 gas hydrate research well, by the Japanese research consortium

T. Uchida[1], R. Matsumoto[2], A. Waseda[1], T. Okui[3], K.Yamada[4], T. Uchida[5], S. Okada[1], and O. Takano[6]

Uchida, T., Matsumoto, R., Waseda, A., Okui, T., Yamada, K., Uchida, T., Okada, S, and Takano, O., 1999: Summary of physicochemical properties of natural gas hydrate and associated gas-hydrate-bearing sediments, JAPEX/JNOC/GSC Mallik 2L-38 gas hydrate research well, by the Japanese research consortium; in *Scientific Results from JAPEX/JNOC/GSC Mallik 2L-38 Gas Hydrate Research Well, Mackenzie Delta, Northwest Territories, Canada, (ed.) S.R. Dallimore, T. Uchida, and T.S. Collett; Geological Survey of Canada, Bulletin 544, p. 205–228.*

Abstract: The JAPEX/JNOC/GSC Mallik 2L-38 gas hydrate research well was drilled to a depth of 1150 m in the Mackenzie Delta, Northwest Territories, Canada, in February and March, 1998. A highlight of the project was the successful retrieval of natural gas hydrate samples in a variety of sediments. A summary is presented of research conducted by the Japanese research consortium led by the Japan National Oil Corporation with participation by ten Japanese companies and institutes. Fingerprints of the gas hydrate crystal structure and the molar ratio of water to guest-gas molecules occupying lattice sites are described for gas-hydrate-bearing samples as obtained by NMR and Raman spectroscopy. X-Ray CT imagery is used to describe the texture and gas hydrate/sediment characteristics of recovered samples during controlled dissociation testing. In addition, inorganic and organic chemical, thermal geophysical, and physical properties are described for key core horizons. Results are also presented documenting the rate of gas hydrate dissociation in drilling fluids with different chemistry including lecithin.

Résumé : En février et mars 1998, le puits de recherche sur les hydrates de gaz JAPEX/JNOC/GSC Mallik 2L-38 a été foré jusqu'à une profondeur de 1 150 m dans le delta du Mackenzie (Territoires du Nord-Ouest, Canada). Un point culminant du projet a été le prélèvement réussi d'échantillons d'hydrates de gaz naturel dans divers sédiments. Les recherches entreprises par le consortium de recherche japonais sous la conduite de la Japan National Oil Corporation et avec la participation de dix entreprises et instituts japonais sont sommairement exposées ci-après. Dans les échantillons contenant des hydrates de gaz, la structure cristalline des hydrates de gaz ainsi que le rapport molaire de l'eau aux molécules de gaz incluses dans la structure cristalline de ceux-ci ont été définis par résonance magnétique nucléaire et par spectroscopie Raman. On a fait appel à l'imagerie tomodensitométrique pour décrire la texture et les caractéristiques des hydrates de gaz et des sédiments des échantillons récupérés au cours d'essais de dissociation contrôlés. Les propriétés chimiques (chimie minérale et organique), les caractéristiques géophysiques et thermiques, ainsi que les propriétés physiques des principaux horizons carottés sont également décrites. D'autres résultats présentés définissent la vitesse de dissociation des hydrates de gaz dans les fluides de forage de diverses compositions chimiques, notamment de la lécithine.

[1] JAPEX Research Center, Japan Petroleum Exploration Company, Ltd., 1-2-1 Hamada, Mihama-ku, Chiba 261-0025, Japan
[2] Geological Institute, University of Tokyo, 7-3-1 Hongo, Bunkyo-ku, Tokyo 113-8656, Japan
[3] Frontier Technology Research Institute, Tokyo Gas Company, Ltd., 1-7-7 Suehiro-cho, Tsurumi-ku, Yokohama 230-0045, Japan
[4] Research & Development Department, Osaka Gas Company, Ltd., 6-19-9 Torishima Konohana-ku, Osaka 554-0051, Japan
[5] Hokkaido National Industrial Research Institute, 2-17-2-1 Tsukisamu-higashi, Toyohira-ku, Sapporo, Hokkaido 062-8517, Japan
[6] Japan National Oil Corporation, Technology Research Center, 2-2 Hamada 1 Chome, Mihama-ku, Chiba 261-0025, Japan

INTRODUCTION

Gas hydrate is a crystalline substance composed of water and natural gas in which a solid water lattice accommodates guest-gas molecules (usually methane) in a clathrate cage. They are known to be widespread in many deep-sea sites worldwide, including regions around the islands of Japan and in several arctic sedimentary basins associated with deep permafrost. While there is abundant indirect geophysical evidence of gas hydrate in these environments, little is known about the geological aspects controlling their occurrence and distribution. However, gas hydrate represents a potentially vast new source of natural gas that may be a future alternative energy resource for Japan, where known fossil-fuel deposits are not sufficient to meet the country's needs. To investigate the potential of natural gas hydrate as an energy resource, Japan embarked on a five-year research program in 1995 with the support of the Ministry of International Trade and Industry (MITI). Led by the Japan National Oil Corporation (JNOC), and with participation by ten oil, gas, and electric companies, research and development projects have been undertaken to investigate various engineering technologies and also conduct scientific studies. The JAPEX/JNOC/GSC Mallik 2L-38 gas hydrate research-well project was conducted in collaboration with the Geological Survey of Canada (GSC) to gain practical field experience and to test various engineering technologies being developed for drilling, coring and producing natural gas hydrate by members of the Japanese consortium prior to a major exploration well planned for offshore Japan in 1999 (Ohara et. al., 1999).

An additional goal was to conduct a scientific study of a permafrost gas hydrate occurrence. The Mallik 2L-38 well, located at the northeastern edge of the Mackenzie Delta, Northwest Territories, Canada, was completed in February and March of 1998, reaching a target depth (TD) of 1150 m. The drill site was selected close to the Imperial Mallik L-38, an industry exploration well drilled in 1972 that documented one of the thickest occurrences of natural gas hydrate known in the area (Bily and Dick, 1974).

This paper presents a summary of the results Japanese collaborators have obtained from various analyses of natural gas hydrate samples and associated gas-hydrate-bearing sediments from the Mallik 2L-38 research well. As such, the paper represents a contribution to the ongoing Japanese research program.

GEOLOGICAL SETTING

The JAPEX/JNOC/GSC Mallik 2L-38 gas hydrate research well was interpreted to intersect Oligocene to Holocene sediments (Fig. 1). A sequence stratigraphy nomenclature has been adopted in the Mackenzie Delta area allowing for description and characterization of these strata (Dixon and Dietrich, 1988; Dixon et al.,1992). The Iperk Sequence was encountered from the surface to a depth of 346 m (all depths were measured from kelly bushing [8.31 m above sea level]) and included Pliocene to Holocene sediments which lie on a marked basal unconformity (Jenner et al., 1999). At the Mallik site, Iperk strata are unconsolidated and are dominated by fluvial deposits representing delta-plain and coastal-plain environments. Near-surface strata include glaciogenic deposits (including thin glacial till and glaciofluvial sand). No hydrocarbon occurrences were documented from the Iperk Sequence. The Mackenzie Bay Sequence, from 346 to 926 m (Jenner et al., 1999), includes Upper Oligocene to Miocene sediments. Strata consist mainly of unconsolidated to weakly cemented sand and silt and no hydrocarbon reserves have been documented. The Kugmallit Sequence, from 926 to 1150 m, consists of Oligocene sediments. Kugmallit strata consist of interbedded, unconsolidated to weakly cemented sand intercalated with silt and mud. A number of regional hydrocarbon reserves are distributed within the Kugmallit sequence, especially in offshore areas.

The base of ice-bearing permafrost is estimated to occur at 640 m based on available well-log information from the Mallik L-38 well. Regional ground-temperature data from nearby wells suggest that near-surface temperatures vary from -6 to -2°C in the upper 100 m of sediment, while below that depth an extensive isothermal section (close to -1°C) may occur (Dallimore and Collett, 1999). In the Mallik L-38 well, ice bonding was thought to be quite variable throughout the sequence with possible talik or ice-free sections. The gas hydrate occurrences in the Mallik L-38 well were described by Bily and Dick (1974) as layered sequences on the basis of electric resistivity and mud gas anomalies. While they originally interpreted an SP transition across several intervals to indicate the presence of free gas in contact with gas hydrate, they admitted that this interpretation was questionable since there was a possibility that the free gas might have formed by gas hydrate dissociation due to drilling disturbance. Dallimore and Collett (1995) indicated that Mallik L-38 encountered about 110 m of gas-hydrate-bearing strata, in ten distinct layers between 819 m and 1111 m, based on well log interpretations. Volumetric calculations, based on well-log response by Collett and Dallimore (1998), suggested that these strata had porosities in the range of 33 to 40% (average 37%) with very high pore-space gas hydrate concentrations ranging from 50 to more than 90% (average 67%) (Uchida et al., 1999).

NATURAL GAS HYDRATE SAMPLES

Approximately 14 m of core in the permafrost zone and 37 m in the gas hydrate zone were retrieved from the Mallik 2L-38 well. About 12 m of gas hydrate layers were actually identified in the zone from 897 to 925 m, beneath the base of the permafrost, where sediments were highly saturated with gas hydrate (Uchida et al., 1999). Typically, gas-hydrate-bearing strata ranged from 10 cm to more than 1.5 m thick with an estimated porosity of 25 to 35%. Visual observations and video records of the character of gas hydrate dissociation were well observed at the well site immediately after hydrate core samples were recovered. Dissociation was also observed under laboratory conditions for about half an hour. The core samples containing gas hydrate from the Mallik 2L-38 well (dominantly pore-space gas hydrate) were the first confirmed samples of natural gas hydrate collected from beneath permafrost in the world.

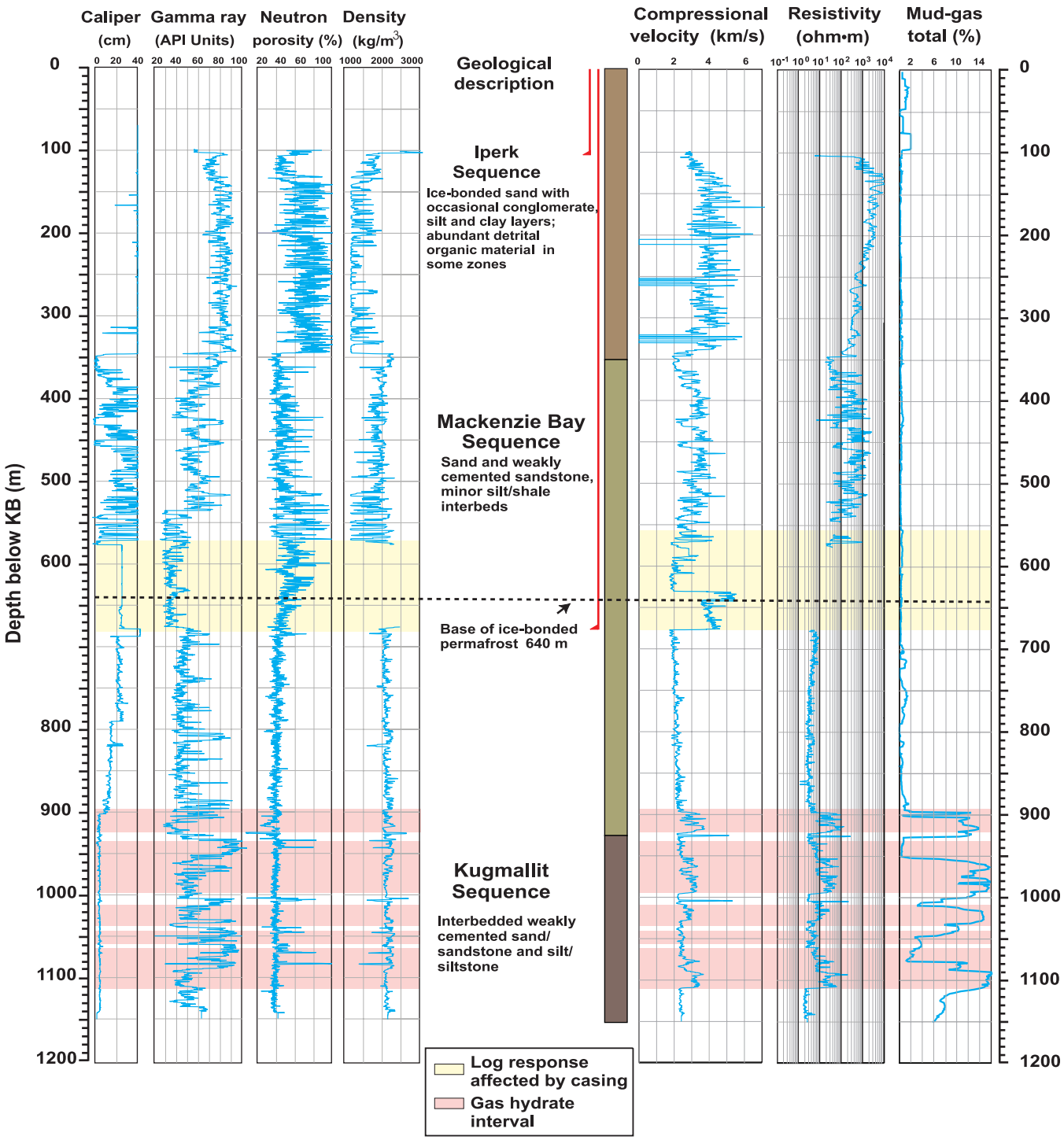

Figure 1. *Lithological units and the geophysical logs of the formations hosting the gas hydrate at the Mallik 2L-38 well site (Dallimore et al., 1999).*

After initial descriptions and testing at the drill site, a limited number of core samples containing gas hydrate were stored in 12 pressure vessels for specialized post-field analyses. The samples were transported to Japan by air, stored in 300 and 920 mL pressure vessels charged with nitrogen gas to 7 MPa pressure. These samples were maintained at -70 to -30°C until analyses were carried out at various JNOC and JAPEX laboratories. After the samples arrived at the laboratory, the pressure of each vessel was checked and gases were collected. Only 2 of 12 vessels had leaked and were at atmospheric pressure. Gas compositions revealed the dominance of methane gas with less than 1% nitrogen. One sample contained 4.86% nitrogen. Visual observations also indicated that the gas hydrate had not significantly dissociated.

CHEMISTRY AND PHYSICS OF GAS HYDRATE

In calculating the amount of methane gas trapped within gas hydrate deposits, one of the most important parameters is the crystal structure of the gas hydrate and the molar ratio of water to guest-gas molecules occupying lattice sites. Core samples of natural gas hydrate were collected from the Mallik 2L-38 research well and transported to Japan for an assortment of analyses including nuclear magnetic resonance (NMR), Raman spectroscopy, inorganic and organic chemistry, as well as physical property and dissociation tests. These analyses provided information on the physical and chemical properties of gas hydrate formation and decomposition and allowed comparison with values from synthetic gas hydrate reported in the literature.

NMR spectroscopy

Nuclear magnetic resonance spectroscopy is a powerful physical method well adapted to a variety of analytical problems in materials characterization. The parameter of interest, the chemical shift, measures the extent to which the magnetic nucleus is shielded by surrounding electrons from an external magnetic field. This parameter is sensitive to local environment, including chemical inequivalence, and in the case of gas hydrate, is sensitive to the nature of the hydrate cage. For optimum resolution and sensitivity in the solid state, the well established cross polarization (CP) technique and magic angle spinning (MAS) techniques were used.

Samples and methods

Sample GH91370 (obtained at a depth of 913.7 m) contained the largest quantity of pure gas hydrate with particles up to about 2 cm in diameter (Uchida et al., 1999) occurring as a pore-space gas hydrate within the intergranular porosity system of granular sand. The hydrate/water ice pore saturation, in this sample, was estimated to be close to 100%. A Bruker AMX-400 NMR spectrometer equipped with a probe for measuring solid substances was used for ^{13}C measurement. The sediment core sample was first crushed in liquid nitrogen and then pure gas hydrate particles were separated from crushed mineral-grain clasts. The collected gas hydrate particles were packed tightly into a zirconia rotor (8 mm in diameter and 10 mm long) and placed in the probe. The rotor was cooled to 203 K (-70°C) and driven at 3000 Hz by dry nitrogen gas. Signals were accumulated 4000 times with the CP/MAS technique and 2000 times with MAS and high-power decoupling for a total of 7 hours of experiment time.

Results and discussion

Both ^{13}C CP/MAS and MAS spectra for the GH91370 sample are shown in Figure 2. Two peaks can be identified at about -3 and -7 ppm, representing methane molecules occupying the small and large cages of the gas hydrate structure, respectively. The ratio of the integrated intensities of the small and large peaks in the spectrum obtained with ^{13}C MAS

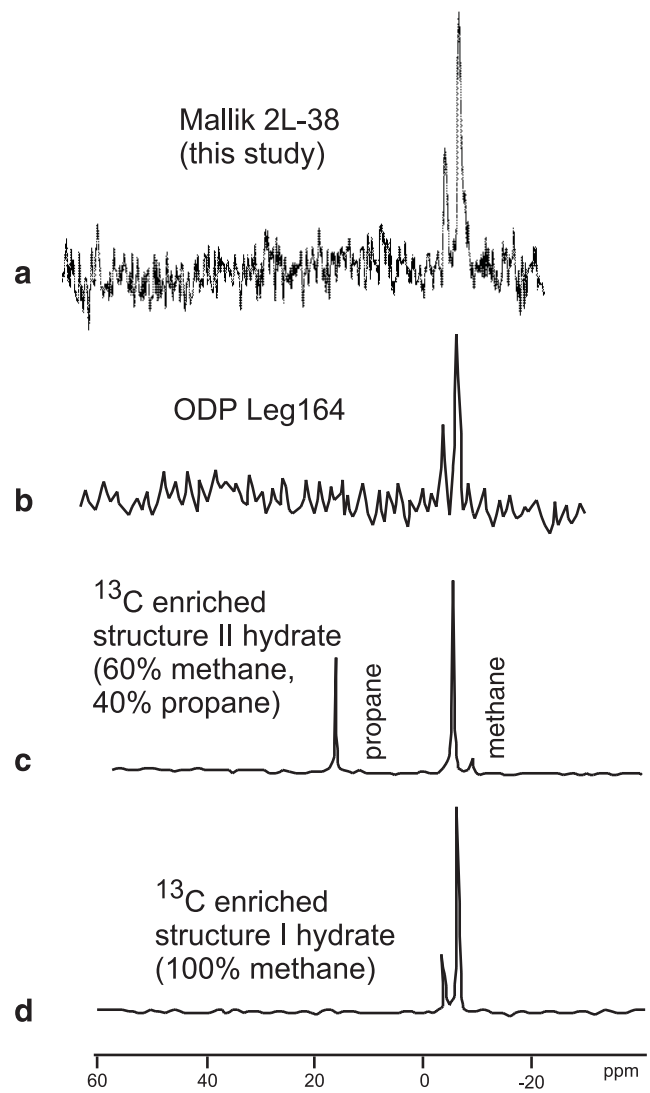

Figure 2. *^{13}C solid CP/MAS NMR spectra for **a)** Mallik 2L-38 sample GH91370, **b)** ODP Leg 164 sample (Uchida et al., 1997), **c)** ^{13}C enriched structure II gas hydrate (Ripmeester and Ratcliffe, 1988), **d)** ^{13}C enriched structure I gas hydrate (Ripmeester and Ratcliffe, 1988).*

and high-power decoupling is somewhat larger than that obtained with the ^{13}C CP/MAS technique. The general intensity distributions for both sets of data are fully consistent with those observed previously for structure I gas hydrate by Ripmeester and Ratcliffe (1988) and from recent samples from the Ocean Drilling Project (ODP) Leg 164 (Uchida et al., 1997; Matsumoto et al., in press).

Raman spectroscopy

Sample and methods

Two specimens were analyzed, GH90475 (collected from 904.75 m) and GH91371 (collected from 913.71 m), and these contained gas hydrate that occurred in intergranular pores in fine-grained and granular sand, respectively. The specimen was placed in a specially designed cryostat for microscopic Raman spectroscopy and temperature was controlled by liquid nitrogen flow in order to maintain a constant temperature of about -50°C. Magnification was about 1000X with a 40X objective lens. The diameter of the incident laser beam was approximately 1 µm. At this magnification it is possible to measure the size of gas hydrate or ice crystals within intergranular pores in the sediment. The Raman spectrometer SPEX RAMALOG-100 was equipped with a 1 m double-dispersed monochromator system for this study. The spectra were recorded using a photomultiplier-tube detector system. The excitation source was an argon-ion laser that emitted a 514.5 nm line and provided about 170 mW. A computer system (SPEX DM1B) provided control of data acquisition for the spectrometer system. Routine calibration of the monochromator was undertaken using neon-lamp radiation. The scattered radiation was collected using a 180° geometry with a slit at 300 µm. The measurements were performed from 2800 to 3000 cm^{-1} in order to measure precisely the guest-molecule vibrations within the gas hydrate. Spectra were collected with a 0.5 cm^{-1} scanning step and 5 second per step integration.

Results and discussion

The Raman spectrum for the sample GH91371 is shown in Figure 3. Two peaks were observed at 2904 and 2915 cm^{-1} with the former being the larger peak. These peaks represent methane's v_1 symmetric bands and indicate that the specimen was almost pure methane gas. Although the v_1 stretching mode of methane vapour is a single peak (~2917 cm^{-1}), this mode has been known to split into two peaks for large and small cages of structure I gas hydrate. This result quantitatively corresponds to Raman spectra from artificial methane hydrate analyses; therefore, it can be confirmed that the gas hydrate samples from Mallik 2L-38 are almost pure methane hydrate. Again, the Raman spectroscopic data agrees well with data for natural gas hydrate obtained from ODP Leg 164 (Matsumoto et al., in press). The Raman spectrum signal was too small to fit statistical curves; therefore, it was impossible to estimate the hydration number of these samples.

In some measurements, a single peak was observed at ~2895 cm^{-1} (*see* Fig. 4). This has not been identified with certainty, but is different from the v_1 stretching of the methane molecule. Compared to other gas hydrate Raman spectra, this peak is close to that of ethane hydrate (2889 cm^{-1}) (Uchida, unpub. data). The concentration of ethane, however, is much smaller than that of methane in the Mallik 2L-38 samples (Table 11). Therefore, if the original composition remains constant, we cannot detect the ethane signal by the Raman spectroscopic analysis. It is possible that the ethane gas was condensed by dissociation, and reformation of gas hydrate occurred due to the lower dissociation pressure of ethane hydrate with respect to methane hydrate at the same temperature.

Gas-to-water ratio

A number of gas hydrate dissociation tests were undertaken at the drill site to investigate the gas-to-water ratio and the hydration number of the gas hydrate.

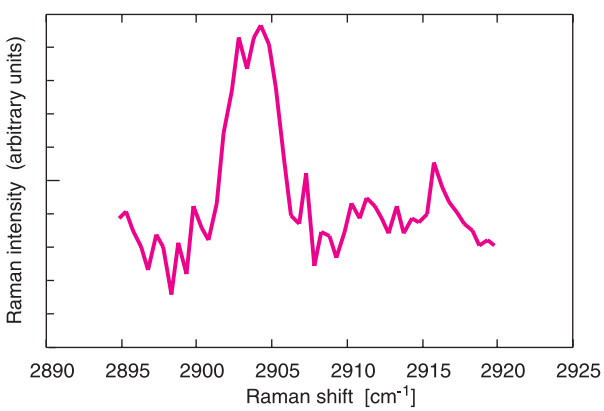

Figure 3. *Raman spectrum obtained from sample GH91371. Two peaks are observed at 2904 and 2915 cm^{-1}, which corresponded to the v_1 symmetric bands of methane in the gas hydrate structure.*

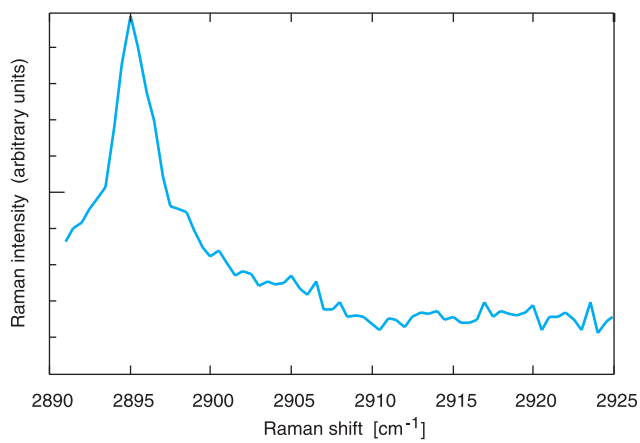

Figure 4. *Raman spectrum obtained from sample GH91371. Another peak is observed at 2895 cm^{-1}, which is close to the value for ethane molecules in the gas hydrate structure.*

Table 1. Results of dissociation tests for gas-hydrate-bearing sand showing gas-to-water ratios.

Sample depth (m)	Temperature (°C)	Pressure (kPa)	Water volume (cm^3)	n (mol)	Gas volume (cm^3)	Gas/water ratio
898.00	11.40	196.133	1.00	0.00216	48.34	48.34
898.00	11.30	176.5197	1.00	0.00194	43.52	43.52
904.75	18.90	529.5591	1.00	0.00567	127.16	127.16
904.75	18.80	117.6798	1.00	0.00126	28.26	28.26
911.75	15.90	627.6256	1.00	0.00679	152.27	152.27
914.60	20.50	225.553	1.00	0.00241	53.86	53.86

Table 2. Thermal conductivity of sample GH90380.

Temperature [°C]	Sample 1 [W/m•K]	Sample 2 [W/m•K]
-30	0.9724	0.8733
-20	0.9937	0.9388
-10	0.9915	1.0251
-5	-	0.9086
0	0.6363	0.9393
5	0.626	-

*pressurized at 10 MPa by CH_4 (methane) gas

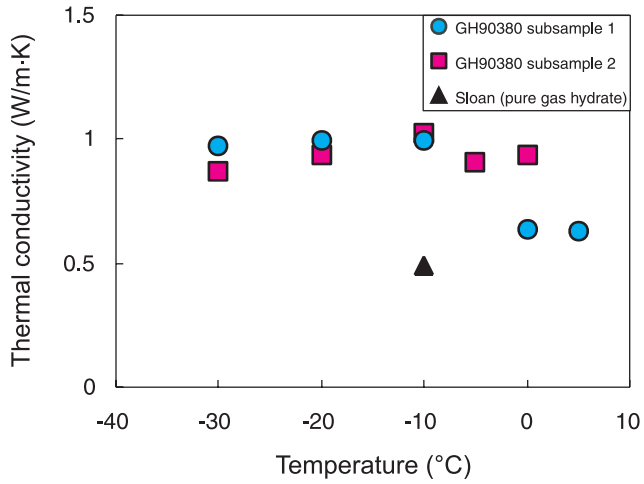

Figure 5. Relationship between thermal conductivity and temperature of Mallik 2L-38 samples and pure gas hydrate sample (Sloan, 1990).

Samples and methods

Six tests were conducted on core samples from gas-hydrate-bearing, fine- to medium-grained sand (Table 1). Small fragments of gas-hydrate-bearing sand (several cm^3) were placed into a small pressure vessel of known volume and then immersed in hot water in order to dissociate the gas hydrate within the sand. The temperature and pressure response of the vessel was monitored, allowing calculation of gas-to-water ratios. The geochemistry of these gases was subsequently analyzed, and is discussed in the 'headspace-gas chemistry' section of this paper.

Results and discussion

Gas-to-water ratio results are shown in Table 1 and range from 44 to 153. Such high gas-to-water ratios may be indicative of structure I hydrate. Unfortunately, the volume of dissociated waters could not be measured precisely because of the difficulty associated with separation of dissociation waters from deformed sediment particles. Thus, these ratios are estimates based on a bulk volume of 3 cm^3 and an average porosity of 30% yielding approximately 1 cm^3 of pore water. For comparison, the pore saturation of gas hydrate is estimated to be greater than 70% throughout most of the in situ gas hydrate layers in Mallik 2L-38 (Miyairi et al., 1999).

Thermal conductivity

Samples and methods

Thermal conductivity measurements were made on the gas-hydrate-bearing sand sample GH90380 (obtained from a depth of 903.80 m) which was divided into two specimens approximately 45 by 25 by 10 mm in size. The sample was fit into a specially designed probe plate apparatus used to measure the thermal conductivity of small samples at high pressure. The measurement system has two types of probes, a plate probe and a needle probe, for the hot-wire method (Yamada and Nakamura, 1997). The plate probe was used because the sample was so stiff. The apparatus was cooled down to -30°C, and then the sample was placed and pressurized to 10 MPa for 4 hours before three measurements were taken (at each temperature) every 4 hours. The results are shown as the average of these three measurements.

Results and discussion

Results from thermal conductivity testing are shown in Table 2 and Figure 5, which includes Sloan's (1990) values. At temperatures between -30 and 5°C, the thermal conductivity of the Mallik samples ranged between 1.0251 and 0.626 W/m•K. The thermal conductivity appears to have increased slightly with temperature between -30 and 0°C and then to have abruptly decreased to 0.65 W/m•K at 0°C. This abrupt decrease may have been caused by the release of free liquid water that lowered the thermal conductivity of the whole system.

Electrical resistivity

Samples and methods

Gas hydrate sample GH90380 (obtained from a depth of 903.80 m; fine-grained sand) was divided into two specimens (~15 mm diameter and 8 mm length) and used to measure electric resistivity. The sample was fit in to a specially designed electrode to measure resistivity of small samples at high pressures.

The apparatus was cooled down to -30°C before the sample was placed into the ring electrode and pressurized to 10 MPa for several hours (Yamada and Nakamura, 1997).

Results and discussion

Resistivity results are shown in Table 3. The Mallik 2L-38 samples do not have similar resistivities to synthetic methane hydrate or pure water ice, but they are similar to the average values for sandstones.

Table 3. Resistivity of sample GH90380.

Temperature [°C]	Resistivity Ω·m
-10	3.58 X 10^3
*pressurized to 10 MPa by CH_4 (methane) gas	

Table 4. Acoustic velocity of sample GH90160.

Temperature [°C]	Vp [m/s]
-6	3110 (1810–4010)
-5	3394 (2890–4110)
*pressurized to 5 MPa by He (helium) gas	

Table 5. Components of the base drilling fluid KCl/polymer.

Water	Starch derivative	Polyanionic cellulose	Xanbis	KCl	KOH
100 g	1.0 g	0.5 g	0.3 g	3.0 g	pH 10.0

Acoustic velocity

Samples and methods

A gas-hydrate-bearing sand, GH901160 (obtained from a depth of 901.60 m) was provided for acoustic-velocity measurements. The sample was shaped to have rectangular faces 40 by 30 by 30 mm to fit into a transducer designed to measure acoustic velocity at high pressure. The apparatus was cooled down to -30°C, and then the sample was pressurized to 5 MPa for several hours before a measurement was taken. The measurement system utilized a sonic wave whose frequency was 28 kHz (Yamada and Nakamura, 1997).

Results and discussion

Measurement results are presented in Table 4 and show averaged temperature values with their acoustic-velocity ranges which are similar to those of synthesized methane hydrate.

Dissociation kinetics

An understanding of the kinetic behaviour of gas hydrate dissociation is especially important for evaluating the resource potential of natural gas hydrate occurrences. In addition to being a factor in assessing the risk of a sudden gas release during exploration or production drilling, dissociation kinetics must be considered when planning a sampling program. However, normal drilling fluids are typically composed of various chemicals, such as salts or glycols, that are well known to reduce gas hydrate stability both within the formation and within core samples. For the Malik 2L-38 well, lecithin was used as an additive to the drilling fluid to stabilize gas hydrate during drilling. Lecithin, which is phospholipid, has been reported elsewhere as an effective drilling fluid additive that keeps gas hydrate stable (Schofield et al., 1997). A series of experiments to evaluate the stability of natural core samples in contact with drilling fluids are described below.

Table 6. Pressure for quick hydrate dissociation at 274 K.

Fluids for dissociation	Synthetic hydrate	Natural hydrate			
		Sample A	Sample B	Sample C	Sample D
	Water	Water	Water+ lecithin	Base drilling fluid (KP)	KP+ lecithin
2.6 MPa	No gas released	No gas released	No gas released	No gas released	No gas released
2.5 MPa	Dissociated	Dissociated	No gas released (at least 2 hrs)	Dissociated	No gas released (at least 2 hrs)
1.6–1.0 MPa			Dissociated		No gas released (at least 2 hrs)
0.7–0.12 MPa					Dissociated

Samples and methods

A core sample from the Mallik 2L-38 well, from 903 m depth (GH90300), was used for testing. The sample consisted of a gas-hydrate-bearing, medium-grained sand, approximately 60 mm in diameter and 100 mm long. The sample, which originally was 276 g, was divided into five specimens (A to E) each between 40 and 70 g. Each specimen was packed in a vinyl bag and placed within a smaller container that was cooled to 253 K and pressurized to 5 MPa by nitrogen gas in a freezer (*see* Table 6).

Lecithin is an insoluble solid in water and therefore comes as a 60 to 65% solution in oil. The product utilized in this testing was provided by Baroid Drilling Fluids, Inc. and is known under the trade name Drilltreat. Water is added to a small amount of the lecithin-oil solution and forms suspension. A 0.6 weight per cent lecithin-water solution and a water-based drilling fluid (Telnite — components are shown in Table 5) were used during drilling of the gas-hydrate-bearing formations.

A schematic diagram of the apparatus used is shown in Figure 6. It consists of a cylinder, whose volume can be adjusted between 0 and 500 cm^3 by moving a piston, connected to an autoclave with a 500 cm^3 volume. The pressure in the system is automatically kept constant during hydrate dissociation by the piston. The rate of dissociation is measured by gas volume withdrawn, as a function of time, at constant pressure. The autoclave and the cylinder were placed in a cooling bath and cooling fluid circulated to keep the temperature constant.

The experimental procedures used to dissociate the gas hydrate are shown in Figure 7. Drilling fluid was cooled in advance and was then introduced into the vessel by a hand-operated pump after each specimen was placed in the vessel and pressurized, by methane gas, to 5 MPa. The sample and the fluid were vigorously agitated to obtain a uniform mixing. The temperature was then raised to 274 K where methane hydrate is stable at 5 MPa. After the temperature became stable, the pressure was decreased to 2.5 MPa, low enough to dissociate hydrate at 274 K.

During these experiments, the amount of gas released and rates of dissociation were monitored successively by measurement of the changes in piston position.

Results and discussion

Gas hydrate dissociation rates within different fluids are listed in Figure 8. The vertical axis designates the ratio of cumulative gas dissociation to total gas released. Five experimental runs were performed for 1) synthetic gas hydrate in water, and 2) natural gas hydrate in water (Run A), 3) natural gas hydrate in water with 0.6 weight per cent lecithin (Run B), 4) natural gas hydrate in base fluid KCl/polymer (Run C), and 5) natural gas hydrate in the KCl/polymer with 0.6 weight per cent lecithin (Run D). Almost no hydrate dissociation was observed, after an hour, in both water with lecithin (Run B) and in KCl/polymer with lecithin (Run D). This may be indicative of the strong effect lecithin has on gas hydrate preservation. Table 6 shows that gas hydrate dissociation did occur at pressures lower than 1.6 MPa in run B, and at 0.7 MPA in run D. This result suggests that dissociation pressures at constant temperatures were influenced by the presence of lecithin, and that lecithin not only affects kinetic

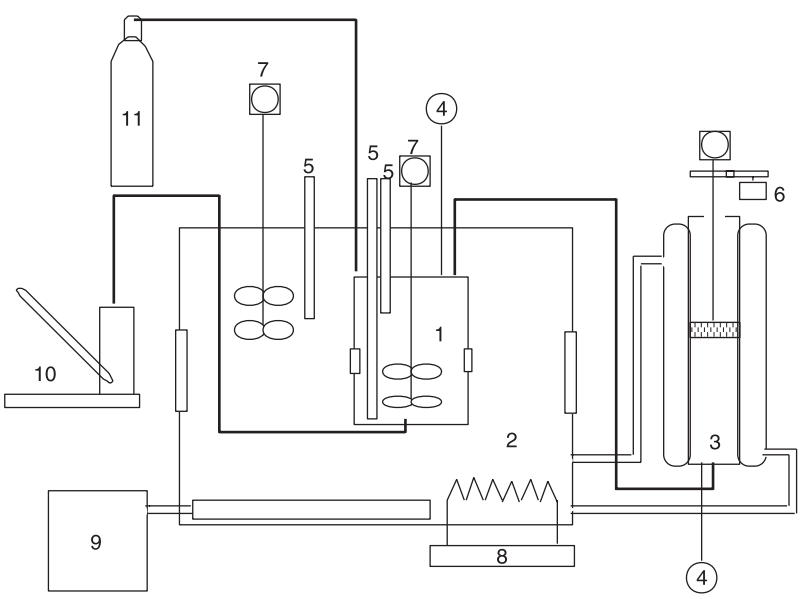

1. Autoclave vessel
2. Glycol-water bath
3. Cylinder
4. Pressure gauge
5. Thermocouple
6. Volumetric sensor
7. Agitator
8. Heater
9. Cooling unit
10. Pump
11. Methane gas

Figure 6.

Schematic diagram of the experimental apparatus.

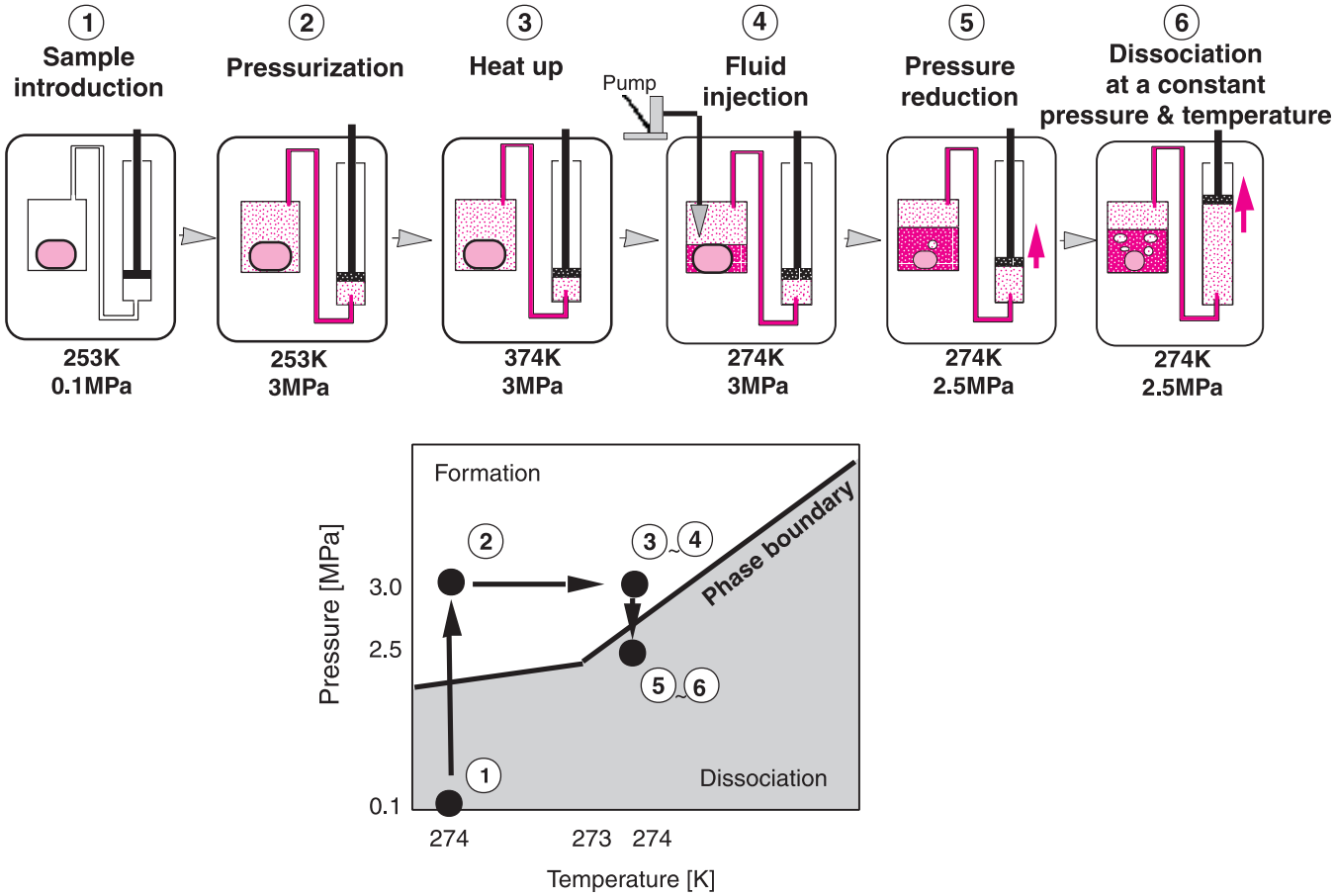

Figure 7. *Experimental procedures for gas hydrate dissociation.*

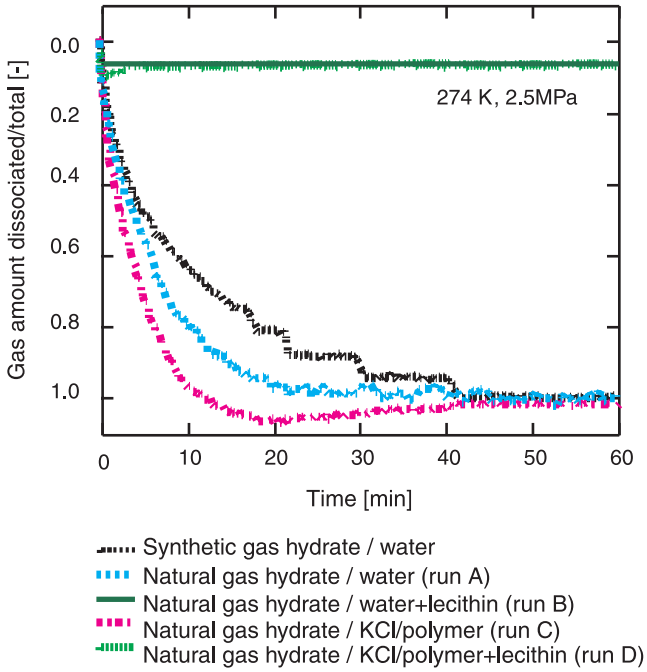

Figure 8. *Dissociation rate of gas hydrate in various fluids.*

properties of gas hydrate dissociation, but also affects thermodynamic properties. These results are quite different from those previously obtained on the effect of lecithin on synthetic pure methane hydrate. Chen et al. (1998) documented a lecithin influence in areas of higher gas hydrate concentration, whereas Okui et al. (1998) observed almost no effect on either thermodynamic or kinetic gas hydrate properties in experimental runs on synthetic hydrate in a 0.6 weight per cent lecithin solution. Figures 9 and 10 plot equilibrium lines and dissociation rates for synthetic methane hydrate in water and in KCl/polymer with 0.6 weight per cent lecithin, respectively.

The only differences between synthetic and natural gas hydrate, in these experiments, were the shapes of the samples and, therefore, the differences in the effects of lecithin may be caused by the shape of the gas hydrate. The natural sediment samples are composed of approximately 5 weight per cent gas hydrate, 15 weight per cent ice, and 80 weight per cent sand particles (Table 7). The amounts of gas hydrate listed in this table are estimated from the quantity of gas released, assuming the water/gas molar ratio is equal to the theoretical value for structure I gas hydrate (5.75). The gas hydrate in these samples fills intergranular pore systems of medium-grained sand, and well disseminated natural gas hydrate should be dispersed as tiny particles when exposed to fluids and

agitated vigorously (Figure 11). The surface area of the gas hydrate is large, and therefore lecithin comes into contact with a significant amount of gas hydrate. In the case of the synthetic gas hydrate, a bulk solid gas hydrate forms, and its relative surface area is much smaller than that of the natural gas hydrate. Lecithin can, therefore, coat the surface of the natural gas hydrate more extensively than on synthetic gas hydrate. This suggests that as pressure decreases, lecithin has a greater effect on natural gas hydrate, which has a larger surface-area-to-volume ratio, than it does on synthetic gas hydrate. It also indicates that lecithin should be used as a standard drilling-fluid additive because it can keep natural gas hydrate stable under what would normally be dissociation temperature and pressure conditions.

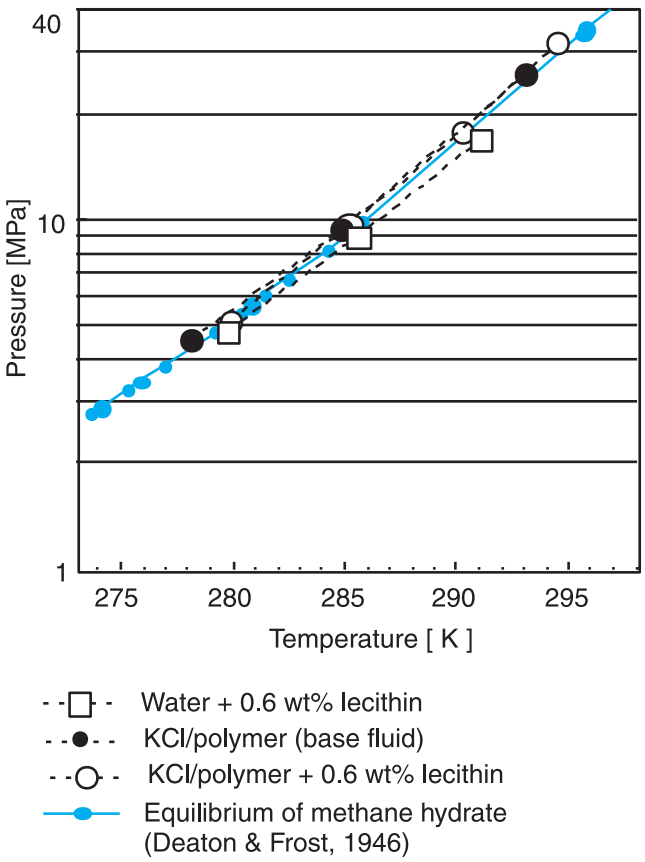

Figure 9. *Formation/dissociation equilibrium of synthetic methane hydrate in KCl/polymer with 0.6 weight per cent lecithin.*

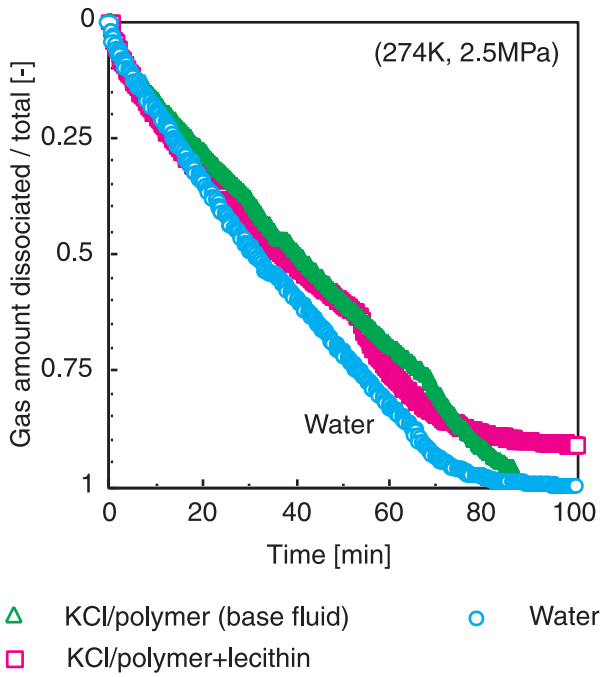

Figure 10. *Dissociation rate of synthetic methane hydrate in KCl/polymer with 0.6 weight per cent lecithin.*

Table 7. Result of dissociation experiments for natural gas hydrate.

	Synthetic gas hydrate	Natural gas hydrate			
		Sample A	Sample B	Sample C	Sample D
Initial sample weight	7.02 g	72.32 g	42.56 g	72.07 g	44.07 g
Total gas amount released	0.00323 mol (0.516 g)	0.0364 mol (0.582 g)	0.0200 mol (0.318 g)	0.0363 mol (0.589 g)	0.0200 mol (0.318 g)
Estimated gas hydrate amount included	3.85 g (55 wt%)	4.35 g (6 wt%)	2.37 g (6 wt%)	4.40 g (6 wt%)	1.76 g (4 wt%)
Sand amount included (remained after dissociation) (dried)	0 g	57.42 g (79 wt%)	33.42 g (78 wt%)	59.22 g (82 wt%)	37.29 g (85 wt%)
Estimated ice amount included	3.17 g (45 wt%)	10.55 g (14.6 wt%)	6.77 g (16 wt%)	8.45 g (12 wt%)	5.02 g (11 wt%)
Exposed fluid for dissociation test	Water	Water	Water + lecithin	Base drilling fluid (KP)	KP+ lecithin

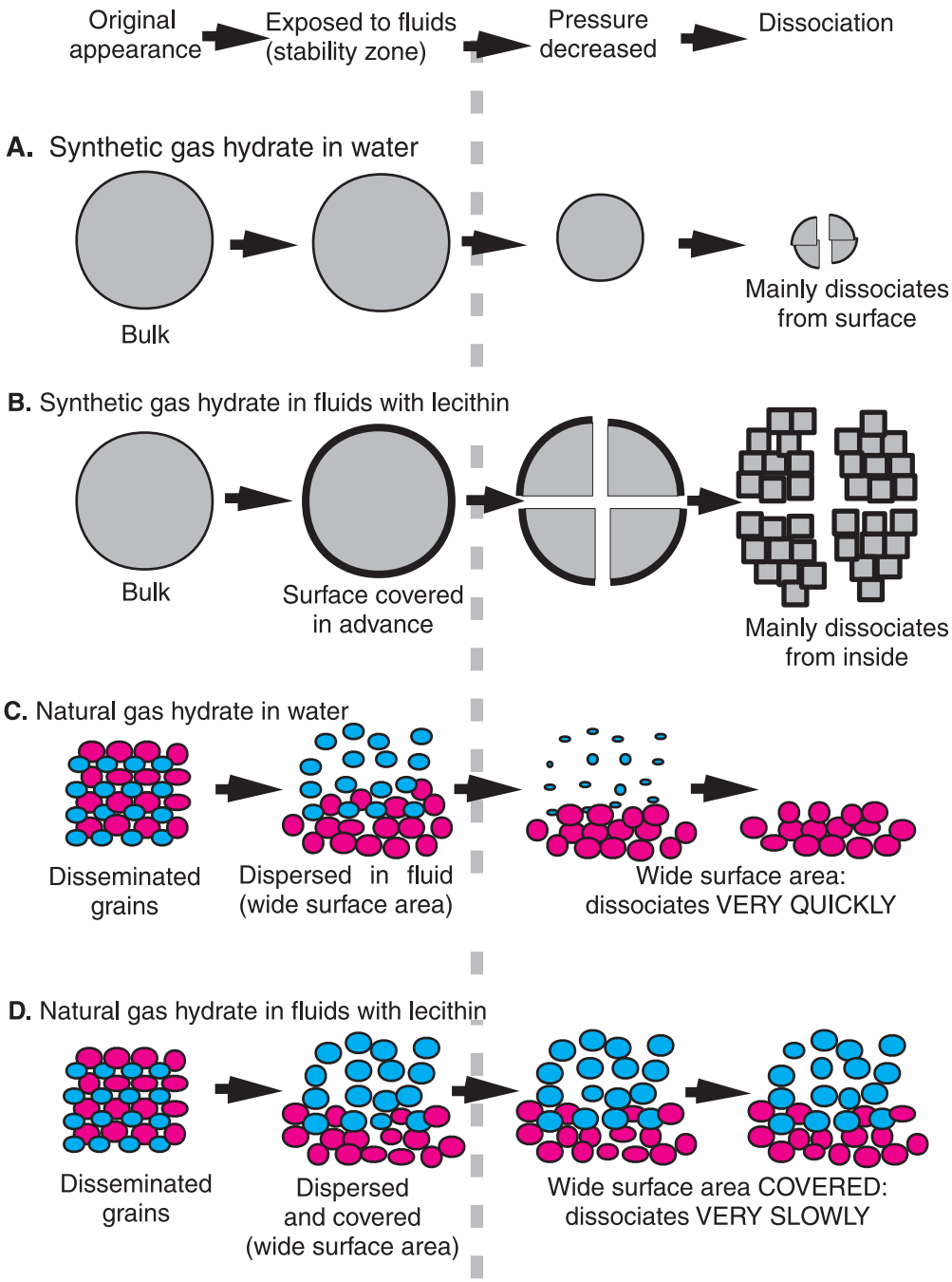

Figure 11. *Influence of gas hydrate shape on lecithin's kinetic preservation effect.*

PHYSICAL PROPERTIES OF SEDIMENTS

Samples and methods

The cored sediment samples, collected from the 887 to 950 m depth interval, are generally unconsolidated sand, silt, and mud with some cemented sandstone around 925 m. Twelve sand, silt, and mud samples were obtained for helium-porosity and mercury-injection tests, and the resulting measurements are shown in Table 8. Nine additional samples are also listed in Table 8 and were provided courtesy of the Geological Survey of Canada (*see* Katsube et al., 1999).

The measurement of helium porosity is a conventionally used method in the petroleum industry, and is usually considered to be very near to the absolute porosity value in a porous substance. Core specimens were subsampled and dried at 80°C for a day before helium-porosity and mercury-porosimetry tests were performed. The pore-size distribution

of samples was determined by mercury-injection porosimetry (e.g. Katsube et al., 1999; Uchida and Tada, 1992). The mercury porosimeter measures the capillary pressure needed to force mercury into accessible pore spaces as well as the volume of mercury injected at each capillary pressure. Assuming that the pores are cylindrical in shape, the capillary pressure can be estimated for equivalent pore sizes simply by using the interfacial tension (about 0.48 N/m) and contact angle (about 139°) of the mercury. Pore-size distributions were derived from the capillary-pressure data.

Results and discussion

The porosity and pore-size-distribution measurements for sand, silt, and mud samples are shown in Table 8. The relationships between porosity, pore size, permeability, and depth are plotted in Figure 12 (nine additional samples were provided by the GSC). Helium and mercury porosities are generally constant (between 25 and 30%), and the mean and median pore radii are more or less constant (<1 µm), except between 905 and 925 m and between 940 and 945 m). Some anomalies occur in the calculated permeability data for these two depth intervals, which coincide with intervals of highly saturated, gas-hydrate-bearing sediment recovery (also seen on downhole well-log data in Fig. 1).

Cumulative pore-size distribution curves for sand, granular sand, silt, and mud are shown in Figures 13 and 14. In both the sandy sediments and muddy sediments, porosities and pore sizes gradually decrease with depth due to diagenetic compaction of clastic sediment particles. Probability curves for sand and granular sand, and for silt and mud are also shown in Figures 15 and 16, and these generally indicate that grain-dominant sand contains small amounts of matrix particles, similar to arenites. In samples from 906.2 and 919.1 m, the intergranular porosity and intragranular porosity are controlled by pore sizes larger than 10 000 nm and smaller than 3 nm, respectively (Uchida and Tada, 1992). The intergranular pore systems of these sandy sediments are expected to be large and permeable enough to permit gas hydrate formation. Probability curves for silt and mud indicate that the typical curves of finer grained sediments are affected by moderate compaction during early diagenesis.

Permeabilities of unconsolidated sediments can be estimated using mercury capillary-pressure data and are especially useful when direct measurements of permeability by fluids such as air cannot be obtained due to difficulties caused by the shape of the unconsolidated samples. Figure 17a shows the relationship between recovery efficiencies (*see* Yamada and Uchida, 1997) and mercury porosities, while Figure 17b shows the relationship between recovery efficiencies and median pore radii, and Figure 17c characterizes the relationship between recovery efficiencies and calculated permeabilities (*see* Yamada and Uchida, 1997). Comparison of these three diagrams demonstrates that the effects of fractures and ink-bottle-shaped pores in the pore systems of rocks and sediments can be evaluated. Two sand samples (collected from 902.20 and 906.20 m) were used to estimate how many ink-bottle-shaped pores occurred in the intergranular pore system. Pore radii can be empirically calculated using the following equation, which combines data from both the pore-size distribution and the grain-size distribution:

$$Pr = 0.46d$$

where Pr is the calculated pore radius and d is the mean grain size of the sediments (Uchida and Tada, 1992). Figure 18 shows a good coincidence between directly measured and calculated values of mean pore size.

Table 8. Pore-size distributions and mercury/helium porosity data for sand and mud.

Depth (m)	Porosity (%)		Permeability (md)	Pore-Size Distribution			
	helium	mercury		mean (µm)	median (µm)	Spec. surf. area (m^2/g)	Calc. perm. (md)
887.20	31.80	37.45		0.295	0.28	5.19	0.19
887.30		24.00		0.397	0.38	10.90	0.33 GSC
891.50	27.60	27.99	2.76	0.088	0.09	7.80	0.03
894.00		30.36		0.167	0.17	6.80	0.08
896.40		29.10		0.158	0.13	20.90	0.08 GSC
896.45		31.08		0.317	0.31	4.97	0.19
896.80		24.50		0.158	0.19	14.80	0.09 GSC
897.10		23.85		0.372	0.50	14.20	0.26 GSC
902.20		32.88		0.735	0.71	4.64	0.59
906.20		42.40		25.05	22.68	13.90	69.50 GSC
919.10		47.40		25.05	25.91	14.40	72.90 GSC
925.90		2.20		0.063	0.07	3.70	0.02 GSC
927.03	29.10	26.83	<0.01	0.099	0.10	8.80	0.03
927.60		25.90		0.158	0.08	14.00	0.10 GSC
929.17	22.20	27.44		0.128	0.13	9.12	0.04
936.30	29.00	25.16		0.097	0.10	6.93	0.03
937.50	30.80	28.10		0.204	0.19	7.04	1.42
943.80	25.20	24.78		1.594	3.62	24.64	1.35
944.10	32.10	20.35		1.873	3.49	29.49	1.02
949.08		25.34		0.135	0.13	6.80	0.05
949.40		27.40		0.397	0.08	20.40	0.25 GSC

Samples marked 'GSC' are courtesy of the Geological Survey of Canada (Katsube et al., 1999).

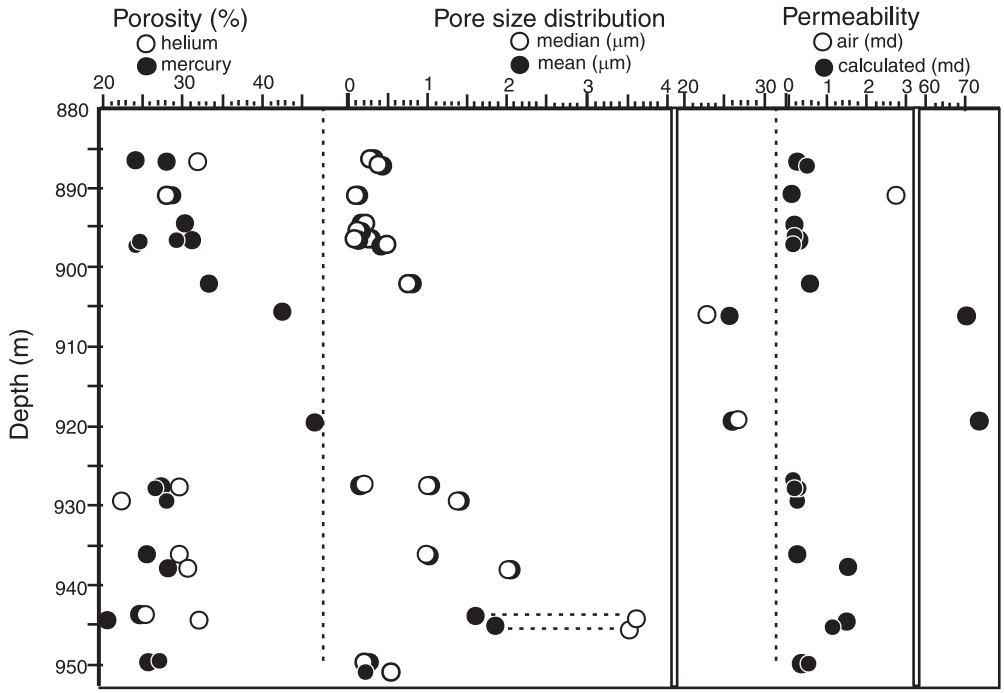

Figure 12. *Relationships of porosities, pore sizes, and permeability with depths.*

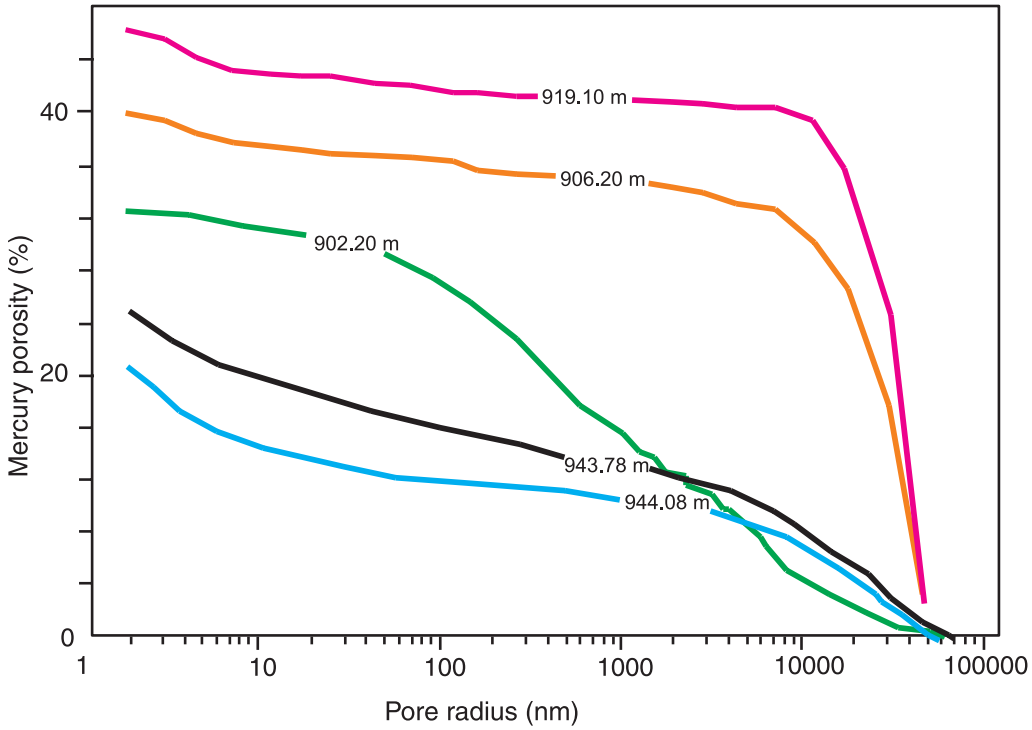

Figure 13. *Cumulative pore-size distribution curves for sand and granular sand.*

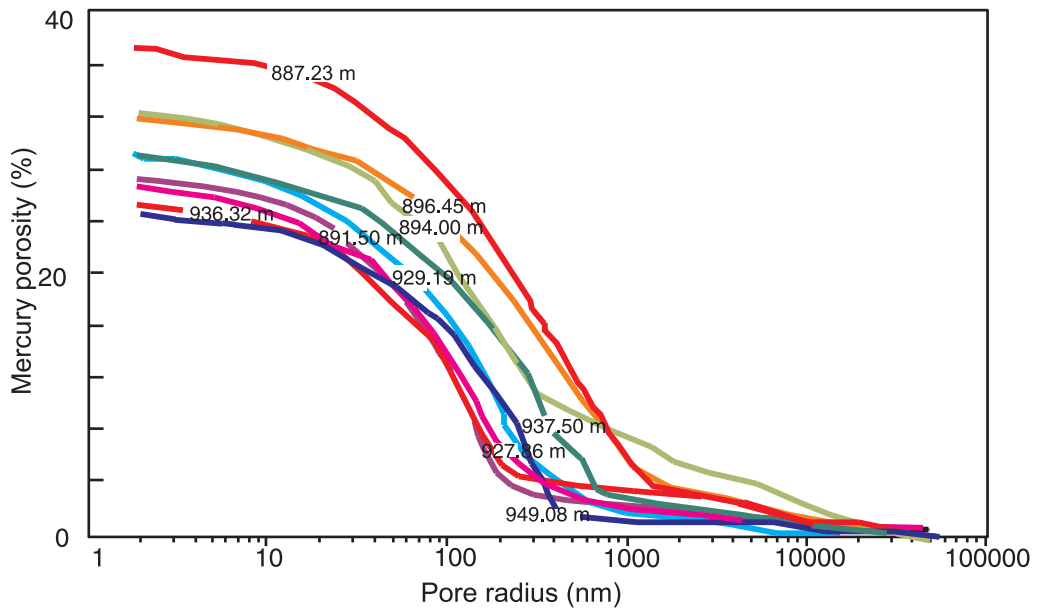

Figure 14. *Cumulative pore-size distribution curves for silt and mud.*

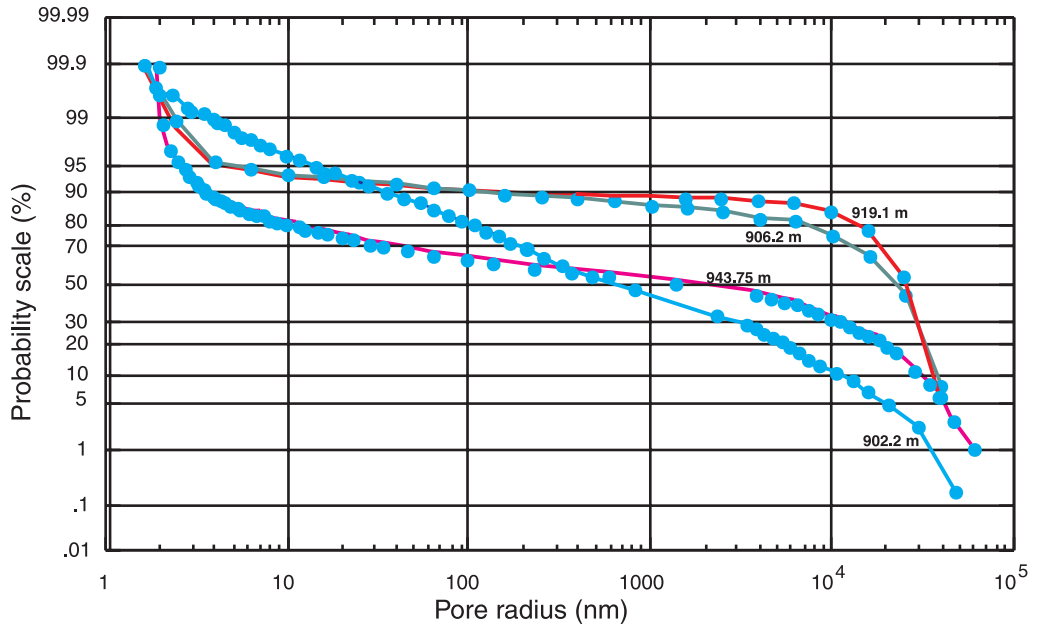

Figure 15. *Probability curves of pore-size distribution curves for sand and granular sand.*

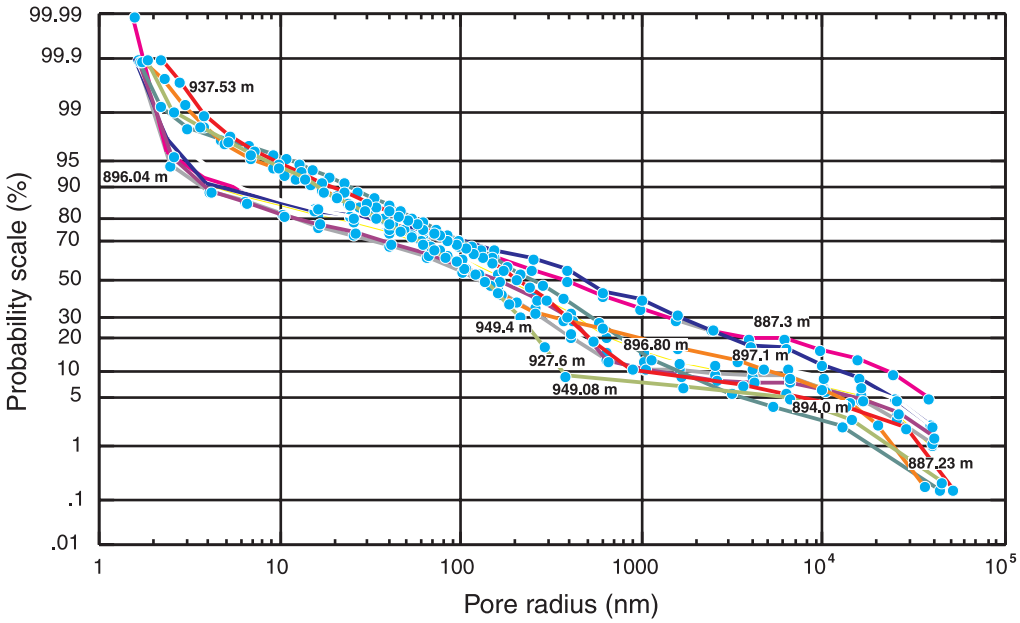

Figure 16. *Probability curves of pore-size distribution curves for silt and mud.*

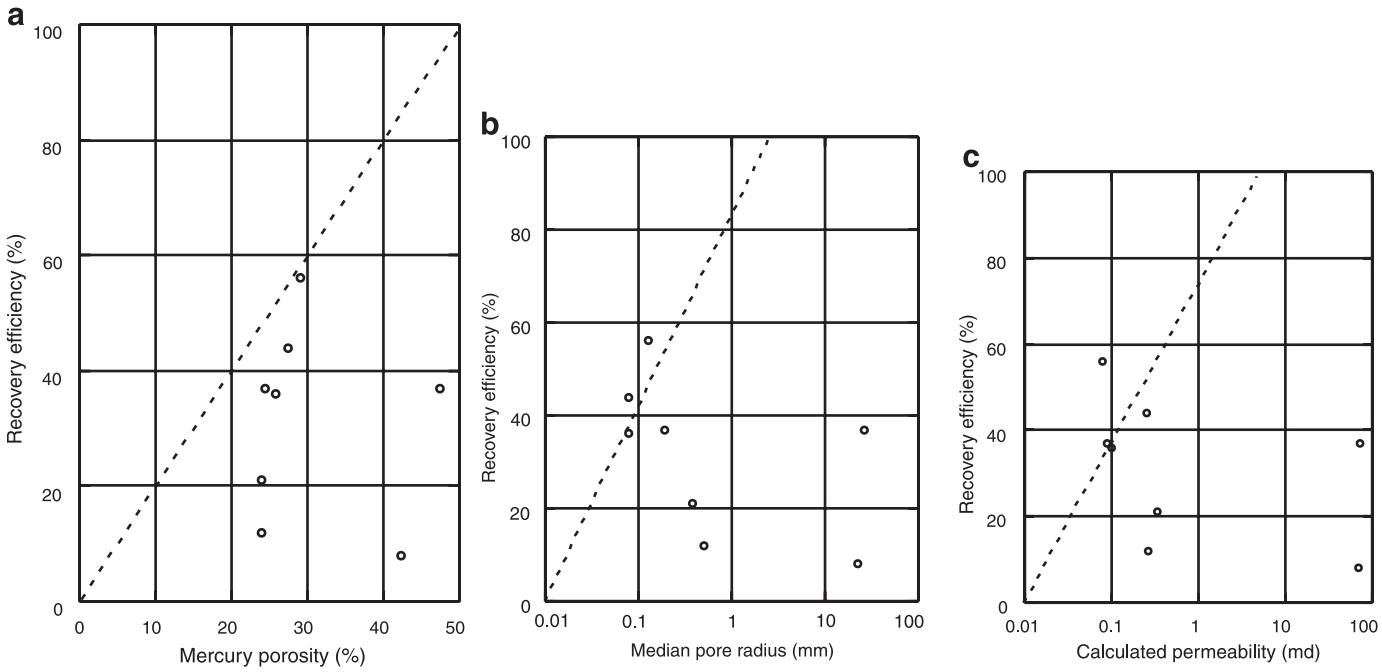

Figure 17. *Relationship of recovery efficiencies with* ***a)*** *mercury porosities,* ***b)*** *median pore radii, and* ***c)*** *calculated permeabilities.*

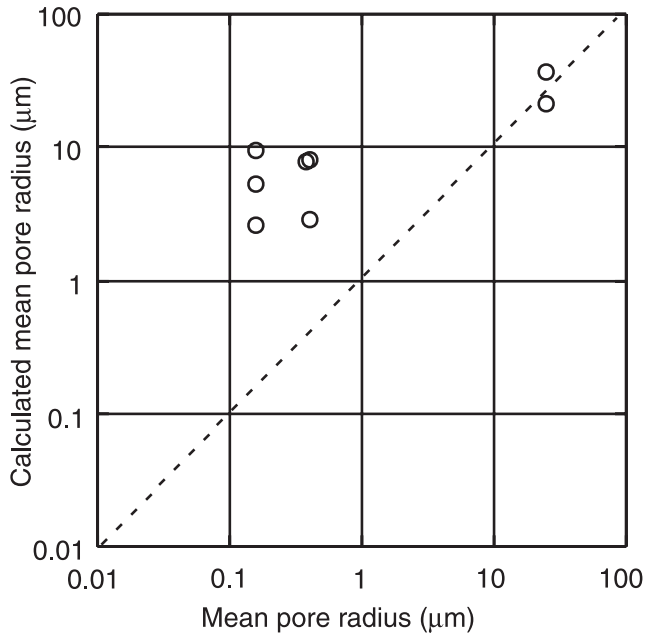

Figure 18. *Relations between mean pore radii and calculated pore radii.*

PORE-WATER CHEMISTRY

Isotope geochemistry of dissociated waters

Samples and methods

Subsamples of dissociation waters, ranging from 5 to 10 mL (sub-1, 2, 3, 4, and 5, respectively), were taken from frozen sediment from a core sample containing gas hydrate, GH91100 (collected from 911.00 m; fine sand), and preserved within a pressure vessel. Each subsample was placed in a small flask in order to evaluate the isotopic equilibration with respect to CO_2 gas. The small flasks containing the subsamples were frozen in liquid nitrogen, evacuated, and then filled with CO_2 gas for C isotopic equilibration reaction with the interstitial waters. The CO_2 flasks were then placed in an incubator, at 25°C for 10 to 15 hours. A second subsample of 80 to 90 mL was squeezed from the sample using a Manheim-type hydraulic squeezer. Approximately 2 mL of interstitial water (IW-1) was obtained during the first hour of squeezing and another 2 mL of interstitial water (IW-2) was obtained during the following 10 hours of squeezing. The standard CO_2-equilibrium method of Epstein and Mayeda (1953), as modified by Matsuhisa and Matsumoto (1985), was used to prepare the CO_2 gas samples from interstitial waters for oxygen-isotope compositional determination. The oxygen-isotope ratio ($^{18}O/^{16}O$) of CO_2 gas was calculated using Finnigan Delta E and Delta S mass spectrometers.

The results are displayed in ‰ delta notation ($\delta^{18}O$ ‰) relative to the SMOW standard. The standard deviation (2-sigma) of independent analyses was 0.01 to 0.05‰, whereas the reproducibility of the measurements was about 0.10‰.

Results and discussion

The results are given in Table 9 and show the $\delta^{18}O$ SMOW of interstitial water samples (IW-1 and IW-2) are -11.94 and -11.69‰, respectively, with an average of -11.82‰. The five subsamples of dissociation waters (sub-1 to sub-5), however, range between -11.48 and -12.03‰ SMOW with a mean value of -11.84 ‰ SMOW, almost identical to that of IW values. This confirms the usefulness of the new CO_2-equilibrium methods applied in this study as a simple technique for the determination of the $\delta^{18}O$ SMOW of interstitial waters, where sample volumes are not large enough to squeeze interstitial waters out.

The $\delta^{18}O$ SMOW value of the interstitial waters of sediment cores from the Mallik 2L-38 research well is anomalously depleted in ^{18}O with respect to the $\delta^{18}O$ SMOW of ocean waters which are ~0‰ SMOW. These apparently anomalous values are believed to be due to the following factors: 1) the ocean waters of the Mackenzie Delta area were diluted by the melting of ^{18}O-deficient ice; 2) the host sediments were not deposited under marine conditions but rather in freshwater fluvial to deltaic environments; or 3) the formation of ^{18}O-enriched gas hydrate, within a closed/semiclosed system, resulted in ^{18}O-deficient interstitial waters. The mean annual $\delta^{18}O$ SMOW value for precipitation (rains and snows) (Yurtsever, 1975) demonstrates that the meteoric waters in the Mackenzie Delta area are strongly depleted in ^{18}O, with $\delta^{18}O$ SMOW values of -20 to -22 ‰. Facies and environmental analysis results are consistent with the oceanic and river-water mixing model during and after the deposition, and during diagenesis of the sediments (Jenner et al., 1999).

Chloride concentration of pore waters

Dissociation of gas hydrate in sediment cores resulted in anomalously low chloride concentrations in pore waters because gas hydrate excludes salt from its crystal lattice and the water derived from the dissociation of gas hydrate is essentially salt-free. The variation in chloride concentrations within the sediment cores is considered to be the most reliable parameter for determination of gas hydrate content in marine sediments (Paull et al., 1996; Matsumoto, in press). Salinity values were determined at the well site by an indirect electric-resistivity technique (Winters et al., 1999), and variability is believed to have been caused by mixing with

Table 9. $\delta^{18}O$ H_2O of gas-hydrate-bearing sand sample GH91100.

Sub-	$\delta^{18}O_{H2O}$ (‰ SMOW)
1	- 12.03
2	- 12.36
3	- 11.48
4	- 11.72
5	- 11.60
mean	- 11.84

freshwater and by water-rock interaction during early diagenesis. This salinity variation within pore waters cannot be due simply to the mixing of freshwater with gas hydrate.

Samples and methods

Pore waters were extracted from small subsamples of 50 to 100 cm^3 taken from 29 sediment core samples (collected from 840.90 to 945.90 m), using a Manheim-type hydraulic squeezer. The volume of extracted water ranged between 0.3 to 5.2 mL depending on the water content and size of core samples. These water samples were stored in vials immediately after extraction. Chloride concentration was determined by an ion-chromatograph IA-100. Standard deviation on these measurements was ~2%.

Results and implications

Results are given in Table 10 and Figure 19, along with the estimated amount of gas hydrate (pore saturation of hydrate) originally contained in the sediment cores. Pore saturations (%) are calculated using the following equation:

$$GH\% = ((Clbg-Clpw)/Clbg)*100$$

where GH% is the pore saturation (volume %) of the gas hydrate, Clbg is the chloride concentration of pristine pore water (baseline value of chloride), and Clpw is the chloride concentration of the samples (measured values). The base line value, Clbg, is tentatively assumed to be 518.75 mmol and was determined to be the mean value of 3 sediment cores (collected from 902.93 to 906.82 m) which were gas-hydrate-free-sediments. Gas hydrate values calculated to be negative are given as zero%.

Table 10. Chloride contents of formation waters in sediment samples and gas hydrate pore saturations calculated from them.

Depth (m)	Cl (mmol)	Gas hydrate (% pore saturation)
840.90	423.70	18.33
886.89	506.63	2.34
890.88	420.59	18.92
891.62	448.80	13.49
892.11	434.70	16.20
899.50	98.73	80.97
902.93	500.42	3.53
905.82	82.93	84.01
905.88	85.19	83.58
906.03	536.53	0.00
906.82	500.99	3.43
921.46	122.99	76.29
927.40	644.85	0.00
935.93	659.24	0.00
936.73	566.43	0.00
937.24	404.51	22.02
937.24	401.69	22.57
937.24	404.80	21.97
937.78	568.12	0.00
938.32	574.05	0.00
945.06	571.79	0.00
945.50	493.37	4.89
946.95	466.29	10.11
947.25	548.94	0.00
947.77	530.61	0.00
949.72	557.12	0.00
950.10	480.96	7.29
951.02	503.24	2.99
945.90	504.94	2.66

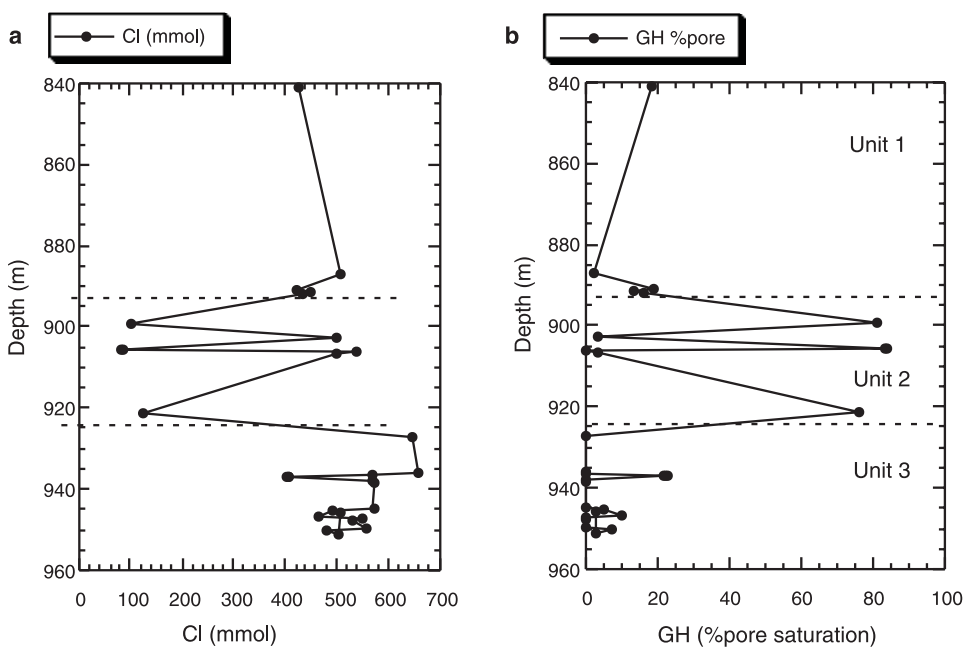

*Figure 19. Depth plot of **a**) chloride contents of formation waters, and **b**) gas hydrate pore saturations calculated from chloride contents.*

The measured interval (840.90 to 945.90 m) was split into three units on the basis of chloride concentrations. The five topmost samples (collected from 840.90 to 892.11 m) range between 423.70 and 506.63 mmol — lower than the mean value for seawater (~560 mmol). These low values may have been caused by gas hydrate dissociation within the sediments, or alternatively, the lower chloride values could be related to the depositional environment of the sediments. Facies analysis of the sediments at the Mallik 2L-38 well site support the idea of a freshwater fluvial to brackish-water deltaic depositional environment (Jenner et al., 1999). The second unit (899.50 to 921.46 m) was characterized by a remarkable fluctuation in the chloride concentration (between 82.93 and 536.53 mmol). Well-site observations confirmed intermittent occurrences of gas hydrate in this interval (between 897 and 923 m, which almost corresponds to this unit). If one assumes that 1) the low chloride concentrations in this unit are caused by the presence of gas hydrate; and 2) the pristine pore waters of the gas-hydrate-free sediments are representative of the mean value (512.6 mmol) of these three data (500.42, 536.53, and 500.99 mmol), then the gas hydrate quantities are estimated to be around 76.3 to 84.0%. These values are surprisingly similar to those estimated from electric logs (Collett et al., 1999; Miyairi et al., 1999). Chloride concentrations from the deepest unit (927.40 to 945.90 m) range between 401 and 660 mmol. Lower chloride values suggest 10 to 20% gas hydrate, and this provides a pristine chloride concentration value of 512.6 mmol. Hypersaline values were calculated at 927.4 and 935.9 m, and may have been caused by residual salt concentrations which were extruded during gas hydrate formation. Alternatively, these fluctuation may have originated from pore waters in hypersaline environments.

In conclusion, the chloride anomaly technique is a reliable and useful tool for estimating the gas hydrate content where base line Cl values are known. In the case of the freshwater to brackish-water sediments, however, the lower chloride values are not necessarily indicative of gas hydrate presence. Sedimentary facies analysis is crucial and must be incorporated into this method.

HEADSPACE-GAS CHEMISTRY

Samples and methods

Twenty-six gas samples were extracted from cuttings between 50 and 1150 m for the analysis of headspace-gas chemistry. Six dissociated-gas samples were released from gas-hydrate-bearing sand between 897 m and 922 m and these were collected at the well site for analysis of gas chemistry (results are listed in Table 11 and 12, respectively).

Cuttings were placed in a can previously prepared with a septa-covered entry port. Distilled water was added to the can and ~200 cm^3 headspace was left at the top. The can was then firmly sealed. In the laboratory, the cans were shaken by ultrasonic waves in order to partition sediment gas into the

Table 11. Molecular composition of hydrocarbons and carbon-isotope composition of methane in headspace-gas samples.

	Depth (m)	O_2 (%)	N_2 (%)	Hydrocarbon (ppm)								C1/ (C2+C3)	$\delta^{13}C$ (‰)
				C1	C2	C3	i-C4	n-C4	i-C5	n-C5	C6+		C1
1	50	2.84	96.29	502	0	0	0	0	0	0	0		
2	100	1.48	95.77	9449	0	0	0	0	0	0	0		-71.7
3	150	3.50	95.74	7571	0	0	0	0	0	0	0		
4	200	2.42	96.91	6635	0	0	0	0	0	0	0		-88.0
5	250	2.69	97.19	1196	0	0	0	0	0	0	0		
6	300	3.21	96.56	2077	0	0	0	0	0	0	0		
7	350	2.90	96.53	3334	0	0	0	0	0	0	0		
8	400	2.88	90.51	55991	0	0	0	0	0	0	0		-83.3
9	450	1.82	97.48	6642	25	20	0	0	0	0	0	148	
10	500	1.39	90.54	11585	27	21	17	0	0	0	0	244	-74.8
11	550	1.43	96.39	5302	27	22	17	0	0	0	0	108	
12	600	1.27	83.75	7785	45	0	14	27	0	0	0	174	
13	650	1.34	88.51	12372	88	35	27	53	57	0	0	101	-61.8
14	700	2.20	97.59	2178	0	0	0	0	0	0	0		
15	750	1.39	95.12	34838	0	0	24	0	0	0	0		-55.5
16	850	3.63	96.01	3563	10	0	12	0	0	0	0	355	
17	900	2.81	96.93	2620	0	15	0	0	0	0	0	180	
18	950	1.99	96.05	19396	122	0	127	12	0	0	0	159	
19	954	2.33	95.35	22759	139	0	201	14	0	0	0	164	-43.9
20	970	1.37	91.44	42078	668	9	327	29	0	0	0	62	
21	980	1.38	92.18	26109	198	0	139	15	0	0	0	132	
22	1000	2.05	96.63	12992	46	0	71	0	0	0	0	285	-43.0
23	1010	1.34	88.53	13924	71	0	250	43	0	0	0	196	-39.6
24	1015	1.25	85.14	25072	68	0	253	41	0	0	0	370	-42.8
25	1100	0.96	66.61	188596	24	0	30	58	0	0	0	7863	-41.0
26	1150	1.28	86.25	53917	27	10	17	48	0	0	0	1447	-43.6

headspace. A portion of the resulting headspace gas was analyzed. Dissociated gases were released from gas-hydrate-bearing sand and collected into gas cylinders after the decomposition of the gas hydrate within the pressure vessel (temperature and gas pressure were recorded).

The hydrocarbon-gas molecular compositions were determined using a Shimazu GC-7A gas chromatograph. Isotopic analyses of methane were conducted separately from the other gas components, using gas chromatography, and subsequently combusted to CO_2 and H_2O, over CuO at 850°C, using a vacuum preparation line (Schoell, 1980). The H_2O was then reduced to H_2 by reaction with zinc in sealed glass tubes at 480°C (Vennemann and O'Neil, 1993). The stable carbon- and hydrogen-isotope compositions of methane were measured using a VG Isotech Sira Series II mass spectrometer. Isotopic ratios are reported in the usual δ-notation, relative to the PDB (Pee Dee belemnite) standard for carbon, and using the SMOW standard for hydrogen. The reproducibility of isotope values are ± 0.15‰ for $\delta^{13}C$ and ±3‰ for δD. The cans were opened and wet samples were collected for total organic carbon (TOC) measurements and Rock-Eval pyrolysis after headspace-gas analyses were complete. Wet sediment samples were dried for 16 hours at 60°C and then crushed and acidified with 6N HCl to remove any carbonate. The TOC of carbonate-free residues were determined using a Yanaco MT-3 CHN Corder and were corrected for carbonate removal. Rock-Eval pyrolysis of whole-rock samples was carried out using a Rock-Eval II as described by Espitalié et al. (1977).

Results and discussion

Carbon-isotope compositions of CH_4 and hydrocarbons indicate that hydrocarbon sources change with depth. Hydrocarbon compositions and $\delta^{13}C$ values of methane are reported in Table 11 and Figure 20. Methane was the only hydrocarbon detected between 50 and 400 m, and the $\delta^{13}C$ values of this CH_4 ranged between -83.3 and -71.7‰, indicating that the methane was mainly produced by microbial activity. Larger hydrocarbon molecules (ethane to pentane) were detected from sediment samples collected from depths greater than 450 m. $\delta^{13}C$ values for CH_4 became heavier with depth (from -75‰ at 500 m to -56‰ at 750 m). In this interval, the origin of gas changed gradually from microbially to thermogenically derived. The $\delta^{13}C$ values of CH_4 from 900 to 1150 m were relatively constant, ranging between -44 and -40‰ and this suggests that gas was generated by thermal decomposition of organic matter. The molecular compositions were relatively rich in methane and depleted in higher hydrocarbons when compared to ordinary thermogenic gases (Figure 21). This may be due to the long migration of gases with depth. Methane is more mobile in sediments than higher

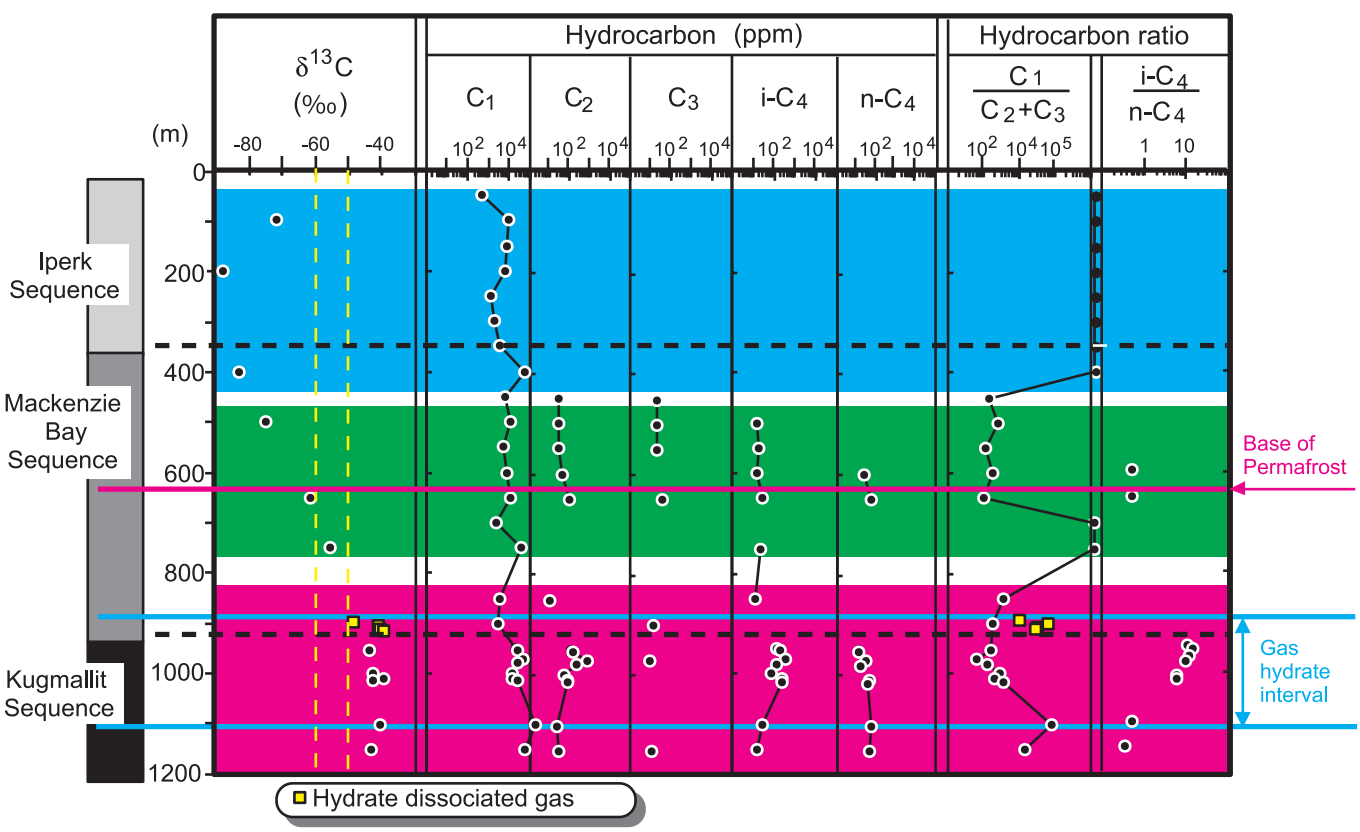

Figure 20. *Depth profile of headspace-gas compositions.*

molecular hydrocarbons; therefore, gas compositions may gradually become more methane-rich during the migration process.

The carbon- and hydrogen-isotope compositions of CH_4 and the molecular compositions of dissociated gas hydrate samples show that the gas trapped within the gas hydrate structure is of thermogenic origin. The hydrocarbon compositions, and the related $\delta^{13}C$ and δD values of methane released from gas-hydrate-bearing sand, are shown in Table 12. The hydrocarbon composition of gas hydrate was almost 100% methane, with only trace amounts of ethane to butane. This composition suggests that the hydrate is structure I. Methane-isotope composition of the gas hydrate sample collected at 898 m was -49‰, and the values of other three samples, collected from 904.75 m to 914.60 m, were around -40‰. These carbon-isotope compositions were identical to those calculated from headspace gases below 950 m (Figure 20). Figure 22 shows hydrogen- and carbon-isotope compositions for methane in the gas hydrate and suggests gas-hydrate-dissociated methane is of thermogenic origin. Headspace gas could not be analyzed for hydrogen-isotope composition due to low methane concentrations. The $\delta^{13}C$ and δD values of methane for sediments from three wells drilled in the Mackenzie Delta at depths shallower than 354 m (Collett and Dallimore, 1997; Figure 22), indicated that shallow methane was generated by microbial activities. The molecular compositions of dissociated gas-hydrate-dissociated gases were enriched in methane when compared to the surrounding headspace gases (Figure 20). The molecular compositions of dissociated gas hydrate more closely reflected in situ free-gas compositions than headspace gas that was adsorbed onto the sediments. Adsorbed gas tends to be enriched in higher hydrocarbons rather than in free gas, since higher hydrocarbons are more easily adsorbed to sediments.

The sediments were generally rich in organic matter throughout the entire well, with the exception of a lean interval between 250 and 450 m (Table 13, Figure 23). The averaged TOC was 3.5% and ranged between 0.3 and 13.5%. Rock-Eval pyrolysis results showed that organic matter was composed of a mixture of Type II marine and Type III terrigenous kerogen (Figure 24). There is a possibility, however, that the pyrolysis results were influenced by mud additives. The cuttings samples contained a lot of jelly-like substances that resembled lecithin, which has a high hydrogen/carbon ratio and a low T_{max} (maximum temperature) value. Small quantities of lecithin may have been missed and would have affected the pyrolysis results. If this was the case, true hydrogen indices could be lower than those calculated and terrigenous matter would have been the main source of organic material.

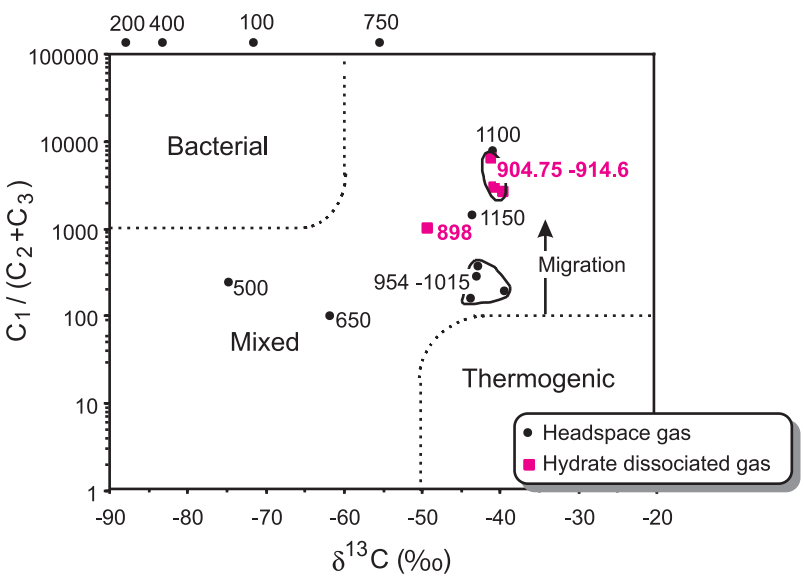

Figure 21.

Interpretive plot of molecular ratios of hydrocarbons vs. carbon-isotope compositions of CH_4 in gas hydrate and headspace gases.

Table 12. Molecular composition of hydrocarbons and carbon- and hydrogen-isotope composition of methane in gas hydrate.

Sample no.	Depth (m)	Gas compositions (vol. %)							C1 / (C2+C3)	$\delta^{13}C$ (‰)	δD (‰)
		C1	C2	C3	i-C4	n-C4	C5+	CO_2		C1	C1
#1	898.00	99.66	0.09	0.00	0.04	0.00	0.00	0.21	1033	-48.7	-231
#2	898.00	99.74	0.02	0.00	0.03	0.00	0.00	0.20	3457		
#3	904.75	99.63	0.02	0.00	0.00	0.00	0.00	0.36	6515	-41.2	-220
#4	904.75	99.68	0.04	0.02	0.00	0.00	0.00	0.26	1548		
#5	911.75	99.87	0.03	0.00	0.00	0.00	0.00	0.10	3017	-40.8	-242
#6	914.60	99.82	0.03	0.01	0.00	0.00	0.00	0.14	2711	-39.6	-230

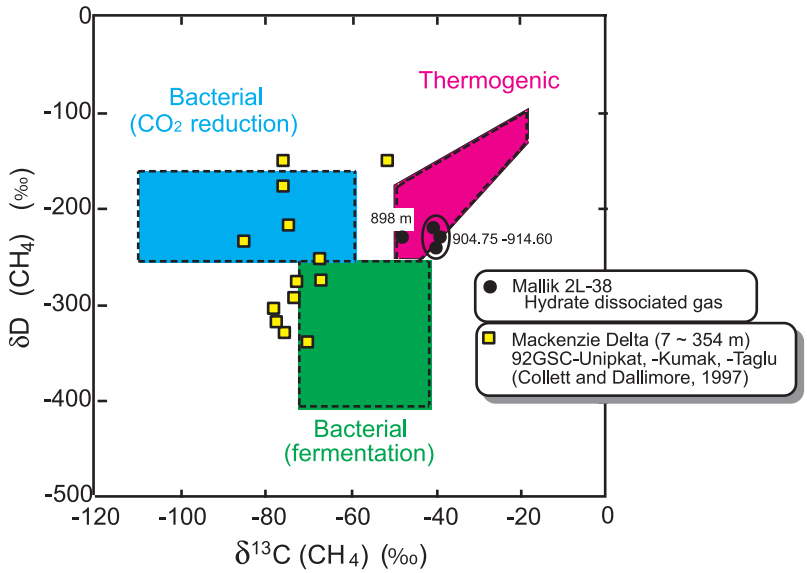

Figure 22.

Interpretive plot of hydrogen- and carbon-isotope compositions of methane in gas hydrate.

Table 13. Total organic carbon (TOC) contents and Rock-Eval pyrolysis results for Mallik 2L-38 samples.

	Depth (m)	Formation	TOC (%)	Tmax (°C)	S1 (mg/g)	S2 (mg/g)	S3 (mg/g)	HI (mg/g)	OI (mg/g)	PI	S1+S2 (mg/g)	S2/ S3
1	50	Iperk	1.43		2.13	3.10	2.58	217	180	0.41	5.23	1.20
2	100	Iperk	2.69		3.06	7.97	11.66	296	433	0.28	11.03	0.68
3	150	Iperk	1.97		1.10	4.68	1.81	238	92	0.19	5.78	2.59
4	200	Iperk	4.11		3.35	11.11	3.01	270	73	0.23	14.46	3.69
5	250	Iperk	0.69		0.38	1.68	0.56	243	81	0.18	2.06	3.00
6	300	Iperk	0.29		0.08	0.35	0.12	121	41	0.19	0.43	2.92
7	350	Mackenzie Bay	0.33	422	0.08	0.34	0.21	103	64	0.19	0.42	1.62
8	400	Mackenzie Bay	0.46	416	0.13	0.72	0.27	157	59	0.15	0.85	2.67
9	450	Mackenzie Bay	0.45	416	0.19	0.62	0.19	138	42	0.23	0.81	3.26
10	500	Mackenzie Bay	1.84	415	0.51	2.13	0.65	116	35	0.19	2.64	3.28
11	550	Mackenzie Bay	2.06		2.36	5.52	2.73	268	133	0.30	7.88	2.02
12	600	Mackenzie Bay	2.96	413	0.54	4.12	2.19	139	74	0.12	4.66	1.88
13	650	Mackenzie Bay	2.57	385	0.66	3.57	1.19	139	46	0.16	4.23	3.00
14	700	Mackenzie Bay	10.57	430	1.35	5.07	2.62	48	25	0.21	6.42	1.94
15	750	Mackenzie Bay	1.61	432	0.56	4.74	2.08	294	129	0.11	5.30	2.28
16	800	Mackenzie Bay	4.91	413	5.16	10.49	4.25	214	87	0.33	15.65	2.47
17	850	Mackenzie Bay	5.60		0.24	0.46	0.30	8	5	0.34	0.70	1.53
18	900	Mackenzie Bay	0.62		0.75	1.29	0.37	208	60	0.37	2.04	3.49
19	950	Kugmallit	4.44	412	2.40	13.24	4.02	298	91	0.15	15.64	3.29
20	954	Kugmallit	5.78	408	3.08	12.22	1.73	211	30	0.20	15.30	7.06
21	970	Kugmallit	6.54	408	2.72	12.27	4.54	188	69	0.18	14.99	2.70
22	980	Kugmallit	3.25	410	0.98	6.41	1.05	197	32	0.13	7.39	6.10
23	1000	Kugmallit	0.93		0.42	1.31	0.42	141	45	0.24	1.73	3.12
24	1010	Kugmallit	2.37	405	0.33	2.38	0.91	100	38	0.12	2.71	2.62
25	1015	Kugmallit	2.21	406	0.42	2.00	0.88	90	40	0.17	2.42	2.27
26	1050	Kugmallit	6.40	410	0.86	10.63	3.00	166	47	0.07	11.49	3.54
27	1100	Kugmallit	13.46	411	2.61	26.47	9.14	197	68	0.09	29.08	2.90
28	1150	Kugmallit	6.66	402	2.42	11.21	1.94	168	29	0.18	13.63	5.78

HI=100xS2/TOC, OI=100xS3/TOC, PI=S1/[S1+S2]
Blanks indicate data point was not determined for broad or distorted S2 peaks.

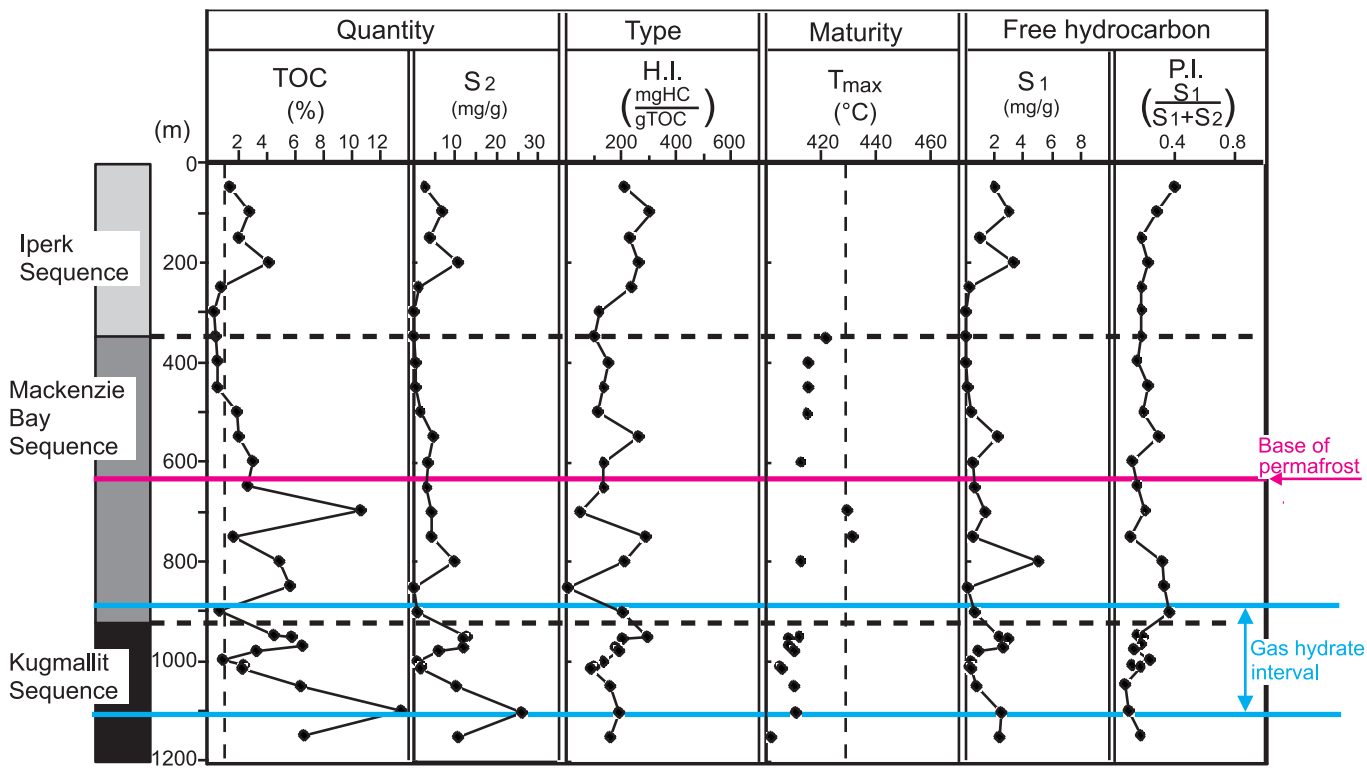

Figure 23. *Depth profile of total organic carbon (TOC) and Rock-Eval pyrolysis results.*

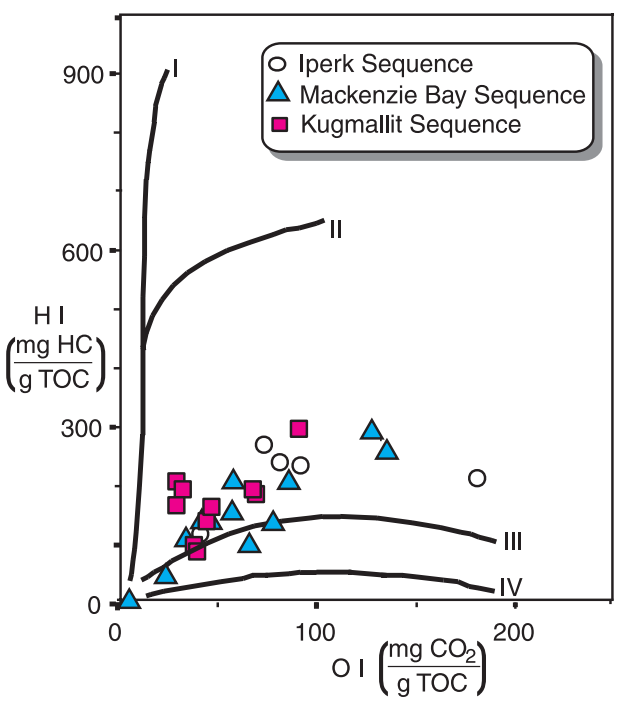

Figure 24. *Hydrogen index (HI) and oxygen index (OI) of organic matter.*

The gas-hydrate-bearing sediments are too immature to have generated hydrocarbons. The Rock-Eval T_{max} values ranged from 385 to 432°C (Table 13, Figure 23). These values showed a wide scatter and may have been slightly affected by mud additives. The entire suite of sediments was interpreted to be immature. The thermogenic gases present in gas hydrate clathrate structures and sediments, therefore, were probably generated in, and migrated from, much deeper, thermally matured sediments.

CONCLUSIONS

The main objective of this paper was to summarize the results Japanese collaborators have produced from analyses of natural gas hydrate and associated sediments obtained from the JAPEX/JNOC/GSC Mallik 2L-38 research well.

The gas hydrate retrieved was mostly pore-space hydrate with small quantities of nodular gas hydrate. Pore-space gas hydrate has not been documented before. The crystal structure of natural gas hydrate and the molar ratio of water to guest-gas molecules occupying lattice sites were investigated by means of NMR, Raman spectroscopy, inorganic and organic chemistry, physical properties, and dissociation tests in hopes that these analyses would supply important information on both the physical and chemical properties of gas hydrate formation and decomposition. The following conclusions were drawn:

1. Nuclear magnetic resonance and Raman spectroscopy analyses on the gas hydrate and sediments from the Mallik 2L-38 research well revealed that all the gas hydrate was of structure I type. The evidence from these spectra agreed well with results published by Ripmeester and Ratcliffe (1988) and ODP Leg 164 (Uchida et al., 1997; Matsumoto et al., in press).
2. The $\delta^{18}O$ SMOW values of the gas hydrate dissociation waters are anomalously depleted in ^{18}O considering that the $\delta^{18}O$ SMOW of ocean waters are nearly 0‰ SMOW. This suggests the ^{18}O-deficient interstitial waters may have been significantly altered by ice-melting or, more likely, were derived from mixing of ocean waters and fresh waters.
3. The thermal conductivity of the Mallik 2L-38 research-well samples range between 1.025 and 0.626 W/m·K at temperatures between -30 and 5°C. The resistivity differs significantly from that of synthetic methane hydrate and pure ice waters, but is similar to that of sandstone. The acoustic velocity is similar to that of synthetic methane hydrate.
4. Lecithin's effect on natural gas hydrate appears to be much greater than its effect on synthetic gas hydrate. Lecithin, as a drilling fluid, should be used since it can keep the natural gas hydrate stable. The particle sizes of gas hydrate and their surface areas may strongly influence the kinetic effect of this additive on gas hydrate dissociation.
5. The gas-to-water ratios calculated at the drill site revealed that the hydrate concentrations were high and that the hydrate saturation exceeded 70% throughout most of the gas hydrate layers.
6. The results of the headspace-gas chemistry analyses indicated that shallow methane was generated by microbial activities and that the thermogenic gases present in the gas hydrate clathrate structures and sediments in the deep parts of the Mallik 2L-38 research well were probably generated in, and migrated from, much deeper, thermally matured sediments.
7. The gases within the gas hydrate are considered to be chiefly of thermogenic origin.

ACKNOWLEDGMENTS

We are indebted to the Geological Survey of Canada and the ongoing research program supported by JNOC and ten oil, gas, and electric companies. Special thanks to J-S. Vincent and P.J. Kurfurst of GSC Ottawa, A. Nakamura and M. Imazato of JNOC, and T. Ohara of JAPEX Drilling Department, who were responsible for carrying out the Mallik 2L-38 gas hydrate research well project successfully. We are also grateful to all colleagues who participated with us on the Mallik project and especially to T.S. Collett of United States Geological Survey at Denver, Colorado, T.H. Mroz of the United States Department of Energy at Morgantown, West Virginia, O. Senoh of JAPEX Exploration Department in Tokyo, T.J. Katsube of GSC, K. Baba and Y. Kajiwara and H. Iwano of JAPEX Research Center, S. Takeya and H. Osada of Hokkaido Univ., S. Konno of Telnite, T. Kawasaki and Y. Maeda of Tokyo Gas. J.A. Ripmeester, S.R. Dallimore, J.F. Wright, and B.E. Medioli are thanked for their efforts to improve the manuscript.

REFERENCES

Bily, C., and Dick, J.W.L.
1974: Natural occurring gas hydrates in the Mackenzie Delta, Northwest Territories; Bulletin of Canadian Petroleum Geology, v. 22, p. 340–352.

Chen, W., Patil, S.L., Kamath, V.A., and Chukwu, G.A.
1998: Role of lecithin in hydrate formation/stabilization in drilling fluids; *in* Proceedings of the International Symposium on Methane Hydrates Resources in the Near Future?, Japan National Oil Corporation – Technology Research Center, Chiba City, Japan, October 20-22, p. 301–310.

Collett, T.S. and Dallimore, S.R.
1997: Characterization of hydrocarbon gases within permafrost, Mackenzie Delta, Northwest Territories, Canada; *in* The Mackenzie Delta Borehole Project, (ed.) S.R. Dallimore and Mathews; Environmental Studies Research Funds, Report No.135, Calgary, Alberta, 1 CD-ROM.
1998: Quantitative assessment of gas hydrates in the Mallik L-38 Well, Mackenzie Delta, N. W. T.; *in* Proceedings of the 7th International Conference on Permafrost, Yellowknife, Canada, Collection Nordicana, Université Laval, p. 189–194.

Collett, T.S., Lewis, R., Dallimore, S.R., Lee, M.W., and Uchida, T.
1999: Detailed evaluation of gas hydrate reservoir properties using JAPEX/JNOC/GSC Mallik 2L-38 gas hydrate research well down-hole well-log displays; *in* Scientific Results from JAPEX/JNOC/GSC Mallik 2L-38 Gas Hydrate Research Well, Mackenzie Delta, Northwest Territories, Canada, (ed.) S.R. Dallimore, T. Uchida, and T.S. Collett; Geological Survey of Canada, Bulletin 544.

Dallimore, S.R. and Collett, T.S.
1995: Intraparmafrost gas hydrates from a deep core hole in the Mackenzie Delta, Northwest Territories, Canada; Geology, v. 23, p. 527–530.
1999: Regional gas hydrate occurrences, permafrost conditions, and Cenozoic geology, Mackenzie Delta area; *in* Scientific Results from JAPEX/JNOC/GSC Mallik 2L-38 Gas Hydrate Research Well, Mackenzie Delta, Northwest Territories, Canada, (ed.) S.R. Dallimore, T. Uchida, and T.S. Collett; Geological Survey of Canada, Bulletin 544.

Dallimore, S.R., Collett, T.S., and Uchida, T.
1999: Overview of science program, JAPEX/JNOC/GSC Mallik 2L-38 gas hydrate research well; *in* Scientific Results from JAPEX/JNOC/GSC Mallik 2L-38 Gas Hydrate Research Well, Mackenzie Delta, Northwest Territories, Canada, (ed.) S.R. Dallimore, T. Uchida, and T.S. Collett; Geological Survey of Canada, Bulletin 544.

Deaton, W.M. and Frost, E.M., Jr.
1946: Monograph 8; United States Bureau of Mines.

Dixon, J. and Dietrich, J. R.
1988: The nature of depositional and seismic sequence boundaries in Cretaceous–Tertiary strata of the Beaufort–Mackenzie Basin; *in* Sequences, Stratigraphy, Sedimentology: Surface and Subsurface, (ed.) D.P. James and D. Leckie; Canadian Society of Petroleum Geologists, Memoir 15, p. 63–72.

Dixon, J., Dietrich, J.R., and McNeil, D.H.
1992: Upper Cretaceous to Pliocene sequence stratigraphy of the Beaufort–Mackenzie and Banks Island areas, northwest Canada; Geological Survey of Canada, Bulletin 407, 90 p.

Espitalié, J., Madec, M., Tissot, B., Menning, J.J., and Leplat, P.
1977: Source rock characterization method for petroleum exploration; *in* Proceedings, 9th Annual Offshore Technology Conference, v. 3, p. 439–444.

Epstein, S. and Mayeda, T.
1953: Variation of oxygen-18 content of waters from natural sources; Geochima et Cosmochimica Acta, v. 4, p. 213–224.

Jenner, K.A., Dallimore, S.R., Clark, I.D., Paré, D., and medioli, B.E.
1999: Sedimentology of gas hydrate host strata from the JAPEX/JNOC/GSC Mallik 2L-38 gas hydrate research well; *in* Scientific Results from JAPEX/JNOC/GSC Mallik 2L-38 Gas Hydrate Research Well, Mackenzie Delta, Northwest Territories, Canada, (ed.) S.R. Dallimore, T. Uchida, and T.S. Collett; Geological Survey of Canada, Bulletin 544.

Katsube, T.J., Uchida, T., Dallimore, S.R., Jenner, K.A., Collett, T.S., and Connell, S.
1999: Petrophyiscal environment of sediments hosting gas hydrate, Mallik 2L-38 gas hydrate research well; *in* Scientific Results from JAPEX/JNOC/GSC Mallik 2L-38 Gas Hydrate Research Well, Mackenzie Delta, Northwest Territories, Canada, (ed.) S.R. Dallimore, T. Uchida, and T.S. Collett; Geological Survey of Canada, Bulletin 544.

Matsuhisa, Y. and Matsumoto, R.
1985: Oxygen isotopic ratios of interstitial waters from the Nankai Trough and the Japan Trench, Leg 87; *in* Initial Reports, Deep Sea Drilling Project 87, (ed.) H. Kagami, D.E. Karig, and W.T. Coulboun; United States Government Office, Washington.

Matsumoto, R.
in press: Gas hydrate estimates from newly determined oxygen isotopic fractionation and $\delta^{18}O$ anomalies of the interstitial waters, ODP Leg 164, Blake Ridge; *in* Proceedings of the Ocean Drilling Project, Scientific Results, (ed.) C.K. Paull, R. Matsumoto, and P. Wallace; Ocean Drilling Project, College Station, Texas.

Matsumoto, R., Uchida, T., Waseda, A., Uchida, T., Takeya, S., Hirano, T., Yamada, K., Maeda, Y., and Okui, T.
in press: Occurrence, structure and composition of natural gas hydrates recovered from the Blake Ridge, ODP Leg 164, Northwest Atlantic; *in* Proceedings of the Ocean Drilling Project, Scientific Results, (ed.) C.K. Paull, R. Matsumoto, and P. Wallace; Ocean Drilling Project, College Station, Texas.

Miyairi, M., Akihisa, K., Uchida, T., Collett, T. S., and Dallimore, S. R.
1999: Well- log interpretations of gas-hydrate-bearing formations in the JAPEX/JNOC/GSC Mallik 2L-38 gas hydrate research well; *in* Scientific Results from JAPEX/JNOC/GSC Mallik 2L-38 Gas Hydrate Research Well, Mackenzie Delta, Northwest Territories, Canada, (ed.) S.R. Dallimore, T. Uchida, and T.S. Collett; Geological Survey of Canada, Bulletin 544.

Ohara, T., Dallimore, S.R., and Fercho, E.
1999: Drilling operations, JAPEX/JNOC/GSC Mallik 2l-38 gas hydrate research well; in Scientific Results from JAPEX/JNOC/GSC Mallik 2L-38 Gas Hydrate Research Well, Mackenzie Delta, Northwest Territories, Canada, (ed.) S.R. Dallimore, T. Uchida, and T.S. Collett; Geological Survey of Canada, Bulletin 544.

Okui, T., Maeda, Y., and Kawasaki, T.
1998: Kinetic control of methane hydrate in drilling fluids; *in* Proceedings of the International Symposium on Methane Hydrates Resources in the Near Future?, Japan National Oil Corporation – Technology Research Center, Chiba City, Japan, p. 293–299.

Paull, C.K., Matsumoto, R., Wallace, P., et al.
1996: Gas hydrate sampling on the Blake Ridge and Carolina Rise; Proceedings of the Ocean Drilling Program, Initial Reports; Ocean Drilling Program, College Station, Texas, v. 164, 623 p.

Ripmeester, J.A. and Ratcliffe, C.I.
1988: Low-temperature cross-polarization/magic angle spinning ^{13}C NMR of solid methane hydrates: structure, cage occupancy, and hydration number; Journal of Physical Chemistry, v. 92, p. 337–339.

Schoell, M.
1980: The hydrogen and carbon isotopic composition of methane from natural gases of various origins; Geochimica et Cosmochimica Acta, v. 44, p. 649–661.

Schofield, T.R., Judzis, A.. and Yousif, M.
1997: Stabilization of in-situ hydrates enhanced drilling performance and rig safety; *in* Proceedings Society of Petroleum Engineers, Annual Technical Conference and Exhibition, San Antonio, Texas, 1997.

Sloan, E.D.
1990: Clathrate hydrates of natural gases; Marcel Dekker, Inc., New York and Basel. p. 641.

Uchida, T. and Tada, R.
1992: Pore properties of sandstones — Part II. Applications for pore-size distribution to natural sandstones; Journal of the Japanese Association for Petroleum Geologists, v. 57, p. 213–222. (In Japanese with English abstract and captions.)

Uchida, T., Dallimore, S. R., Mikami, J., and Nixon, F.M.
1999: Occurrences and X-ray computerized tomography (CT) observations of natural gas hydrate, JAPEX/JNOC/GSC Mallik 2L-38 gas hydrate research well; *in* Scientific Results from JAPEX/JNOC/GSC Mallik 2L-38 Gas Hydrate Research Well, Mackenzie Delta, Northwest Territories, Canada, (ed.) S.R. Dallimore, T. Uchida, and T.S. Collett; Geological Survey of Canada, Bulletin 544.

Uchida, T., Yamamoto, J., Okada, S., Waseda, A., Baba, K., Okatsu, K., Matsumoto, R., and the Shipboard Scientific Party of ODP Leg 164
1997: Methane hydrates in deep marine sediments — X-ray CT and NMR studies of ODP Leg 164 hydrates; Chishitsu News (Journal of the Geological Survey of Japan), v. 510, p. 36–42. (In Japanese.)

Vennemann, T.W. and O'Neil, J.R.
1993: A simple and inexpensive method of hydrogen isotope and water analyses of minerals and rocks based on zinc reagent; Chemical Geology, v. 103, p. 227–234.

Winters, W. , Dallimore, S.R. , Collett, T.S., Katsube, T.J., Jenner, K.A., Cranston, R.E., Wright, J.F., Nixon, F.M., and Uchida, T.
1999: Physical properties of sediments from the JAPEX/JNOC/GSC Mallik 2L-38 gas hydrate research well; *in* Scientific Results from JAPEX/JNOC/GSC Mallik 2L-38 Gas Hydrate Research Well, Mackenzie Delta, Northwest Territories, Canada, (ed.) S.R. Dallimore, T. Uchida, and T.S. Collett; Geological Survey of Canada, Bulletin 544.

Yamada, K. and Nakamura, K.
1997: Synthesis of methane hydrate for measurement of physical properties; *in* Proceedings of International Workshop on Gas Hydrates Studies (2nd Joint Japan-Canada Workshop at Tsukuba, Japan, p. 124–153.

Yamada, Y. and Uchida, T.
1997: Characteristics of hydrothermal alterations and secondary porosities in volcanic rock reservoirs, Katakai Gas Field; Journal of the Japanese Association for Petroleum Geologists 62, 311–320. (in Japanese with English abstract and captions)

Yurtsever, Y.
1975: Worldwide survey of stable isotopes in precipitations; Rept. Sect. Isotope Hydrol., IAEA, Nov. 1975, 40 p.